*Environmental Epigenetics*, 2026, **12**(1), 1–21
https://doi.org/10.1093/eep/dvag030
Published: 14 August 2026
**Research article**

ENVIRONMENTAL EPIGENETICS OXFORD

# Investigation of psychosocial stress and DNA methylation in genes related to immune response, metabolism, and calcium signaling among African American and White middle-aged adults

Kumaraswamy Naidu Chitrala[1,2], Danielle L. Beatty Moody[3], Nicolle A. Mode[2], Botong Shen[2], Nicole Noren Hooten[2], Alan B. Zonderman[2], Ngozi Ezike[2], Michele K. Evans[2,*]

[1]Department of Engineering Technology, College of Technology, University of Houston, Sugar Land, TX 77479, United States
[2]Laboratory of Epidemiology and Population Sciences, National Institute on Aging, National Institutes of Health, Baltimore, MD 21224, United States
[3]School of Social Work, Rutgers University, New Brunswick, NJ 08901, United States

*Corresponding author. Laboratory of Epidemiology and Population Sciences, National Institute on Aging, National Institutes of Health, NIH Biomedical Research Center, 251 Bayview Boulevard, Suite 100, Room 4C-222, Baltimore, MD 21224, USA. E-mail: me42v@nih.gov

## Abstract

**Chronic psychological stress is an environmental factor associated with chronic disease risk and health disparities. Since environmental stressors alter gene expression and physiologic responses through epigenetic mechanisms, perceived discrimination (PD), or the subjective experience of receiving negative treatment related to personal characteristics may influence DNA methylation (DNAm) of CpGs within genes linked to chronic disease. Using the Illumina 850K EPIC chip and psychosocial stress-associated discrimination scales, including the lifetime, racial, and everyday discrimination scales, we identified novel CpGs and differentially methylated positions (DMPs) associated with PD in the context of age, sex, and poverty status among African American and White adults and ones that overlap previous findings of differentially methylated sites (or genes) with discrimination, inflammation, and chronic disease. Ingenuity Pathway Analysis identified several pathways associated with the DNAm patterns and PD with age, sex, and/or poverty status. With age, the white adipose tissue browning pathway was activated among African American participants. This was related to the differential methylation found in the *CACNA1H*, *PRDM16*, and *BDNF* genes. Among White participants, the opioid signaling pathway was activated and significantly enriched for the genes *FGR*, *POMC*, and *RPS6KA2.* Additionally, CpG sites associated with PD among White participants with poverty status revealed that the netrin signaling, opioid signaling, and calcium signaling pathways were activated and significantly enriched for differentially methylated genes, including *NFATC1 and NFATC2.* The identified novel DNAm genes associated with PD transduce effects through biological pathways related to inflammation and immune response, white adipose tissue browning, and calcium signaling.**

***Keywords*** **psychosocial stress, DNA methylation, race, health disparities, minority health, aging, social determinants of health, epigenetics**

## Introduction

Psychosocial stress adversely affects health and health outcomes. These stressors cause biological and physiological responses that are thought to contribute to health disparities and the accelerated aging phenotype [1]. Recent data suggest that perceived discrimination (PD) is a psychosocial stressor that contributes to health disparities in age-associated chronic diseases. For example, discrimination has been associated with cardiovascular disease risk factors [2, 3], metabolism [4], cognition [5, 6], and brain health [7]. Despite accumulating evidence that discrimination adversely affects mental and physical health, the underlying biological mechanisms that drive these effects are largely unknown. One possible biologic transduction pathway considered has been genome-based. There have been some genome-wide associ-

**Received:** 11 September 2025. **Revised:** 31 July 2026. **Accepted:** 9 August 2026

ation studies and related genetic studies examining individual experiences of psychosocial stress. There is evidence in the literature demonstrating that psychosocial stress is associated with alterations in DNA methylation (DNAm) status [8, 9] and the effects of genetic variants around single-nucleotide polymorphisms on clinical outcomes. Epigenetic mechanisms may be one biologic pathway through which psychosocial stressor discrimination may cause physiological changes. These mechanisms can alter transcriptional programs without changing DNA sequence and are influenced by environmental, lifestyle, and psychosocial factors [10–12]. Of the epigenetic mechanisms, DNAm is the most well-studied epigenetic modification and occurs at CpG sites in the genome. There is substantial evidence that DNAm is influenced by environmental exposures, including lead, diet, and polychlorinated biphenyls, and psychosocial stressors such as maternal deprivation, exposure to early life adversity, and violence (for review, see [13, 14]). Few studies have examined the effect of discrimination on DNAm. In African American youth, experiencing high levels of perceived racial discrimination with a less supportive family environment led to accelerated epigenetic aging [15]. On the contrary, exposure to perceived racial discrimination coupled with a strong supportive family environment mitigated these effects on epigenetic aging [15]. Major life discrimination was associated with nine different DNAm CpG sites in African American mothers enrolled in the Intergenerational Impact of Genetic and Psychological Factors on Blood Pressure (InterGEN) study [16]. Discrimination was also associated with DNAm of select genes in pregnant Latina women and in Ghanaian migrants [17, 18]. These studies suggest a link between discrimination and DNAm. Nevertheless, there is still much to learn about the different experiences of discrimination and their influence in both African American and White adults.

The psychosocial stressor discrimination is multidimensional in nature, via race or gender [19] and can be experienced both short term (everyday) and long term (lifetime) [20]. Different forms of PD have different health-related consequences given the different timescales and nature of the experiences, acute versus chronic exposure. Work from the Forde laboratory compared the risk of developing hypertension among African Americans who reported exposure to discrimination on both the everyday and lifetime discrimination scales. Only the lifetime discrimination scale predicted the risk of developing hypertension [21] . Measures of psychological stress are influenced by endogenous and exogenous factors. These factors may include exogenous environmental-based exposures like housing, occupation, social support, and educational opportunities, as well as endogenous factors like mental health, health behaviors, and coping measures. These factors operate and interact at many levels. Therefore, in this study, we primarily explored the impacts of interpersonal or individual-level PD as measured by the lifetime discrimination scale on DNAm in a cohort of African American and White adults. Secondarily, we explored the relationship of everyday, racial, and gender discrimination with DNAm in this cohort. Here, we identified novel CpG sites and investigated previously reported CpG sites associated with psychosocial stress. We also evaluated the differentially methylated signatures associated with psychosocial stress versus the differentially methylated signatures associated with chronic diseases. Assessing a multitude of discrimination measures in relation to DNAm can provide a broader picture of the impact and complexity of this psychosocial stressor on the epigenome and whether these changes overlap with those observed in chronic disease.

# Results

## Study baseline characteristics

A cohort of 467 participants had both DNAm and complete psychosocial stress scale data. Of these, 51% were African American adults and 49% were White adults (Table S1 panel A). A fraction of both African American and White participants reported experiencing lifetime or racial discrimination. Both African American (50.0%) and White (49.0%) participants ($n = 228$) reported (Ldisc+) (Table S1 panel B). African American participants more frequently reported Ldisc compared to White participants (32.7% and 16%, respectively; $P$-value $< .0001$). Analysis of Rdisc revealed that 36.7% ($n = 172$) reported experiencing racial discrimination (Rdisc$^+$) (Table S1 panel C). While both African American and White participants reported experiencing racial discrimination, more African American participants reported Rdisc compared to White participants (28.0% to 8.7%, respectively; $P$-value $< .001$). Therefore, in this cohort, African Americans more frequently reported Ldisc and Rdisc forms of PD, but it is also notable that White participants reported both lifetime and racial discrimination. There were no significant differences between African American and White participants in age, race, sex, or poverty status for the sources of discrimination (Sdisc), gender (Gdisc), everyday (Edisc), and coping with discrimination (Cdisc) scales (data not shown).

## Race stratified age, sex, and poverty status adjusted analysis of DNA methylation and lifetime discrimination with age, sex, and poverty status

Among African American participants, there were 60 CpG sites significantly methylated in the age-adjusted analysis (Model 1). The top 10 hypermethylated CpG sites shown in Fig. 1A (red bars) are associated with the following genes: *PRDM16*, *GFI1*, *NOD1*, *PALM*, *PITX2*, and *CD300A*. The top 10 hypomethylated CpG sites shown in Fig. 1A (green bars) are associated with the following genes: *ARHGAP26*, *DTHD1*, *NFATC2*, *FAM160B1*, *ZSWIM6*, *MBP*, *PTPRN2*, *PTPRE*, *DYSF*, and *SNCA*. The most differentially methylated CpG sites are listed in Table 1 (top panel).

Among White participants, 94 CpG sites were significantly methylated in the age-adjusted analysis. The top 10 hypermethylated CpG sites shown in Fig. 1A-second column (red bars) are associated with the following genes: *SORCS1*, *CD44*, *NR3C1*, *PITX2*, *AHRR*, *PRDM16*, *ZXDC*, *PTPRN2*, *PTPRE*, *DYSF*, and *SNCA*. The most differentially methylated CpG sites are listed in Table 1 (top panel).

Among White participants, 94 CpG sites were significantly methylated in the age-adjusted analysis. The top 10 hypermethylated CpG sites shown in Fig. 1A-second column (red bars) are associated with the following genes: *SORCS1*, *CD44*, *NR3C1*, *PITX2*, *AHRR*, *PRDM16*, *ZXDC*, *PTPRN2*, *HOXD3*, and *ATP9A.* The green bars in Fig. 1A (second column) show the top 10 hypomethylated CpG sites that are associated with the following genes: *MUC5B*, *AHRR*, *FAM49B*, *NAALADL2*, *TOMM20*, *JARID2*, *CLYBL*, *DSE*, *SMG6*, and *POU6F2*. The most differentially methylated CpGs are listed in Table 1 (bottom panel).

In the sex-adjusted analysis (Model 2), we identified 48 significantly methylated CpG sites. Among African American individuals, the top 10 hypermethylated CpG sites as shown in Fig. 1B (red bars) are associated with the following genes: *PRDM16*, *FGR*, *MYO5C*, *GFI1*, *SLC7A11*, *PTPRN2*, *RUNX1*, and *ZNF423.* The top 10 hypomethylated CpG sites shown by the green bars in Fig. 1B are associated with genes *NPAS3*, *PTPRN2*, *RSPO3*, *FAM160B1*, *PTPRE*, *TSC2*, and *RASIP1*. The most

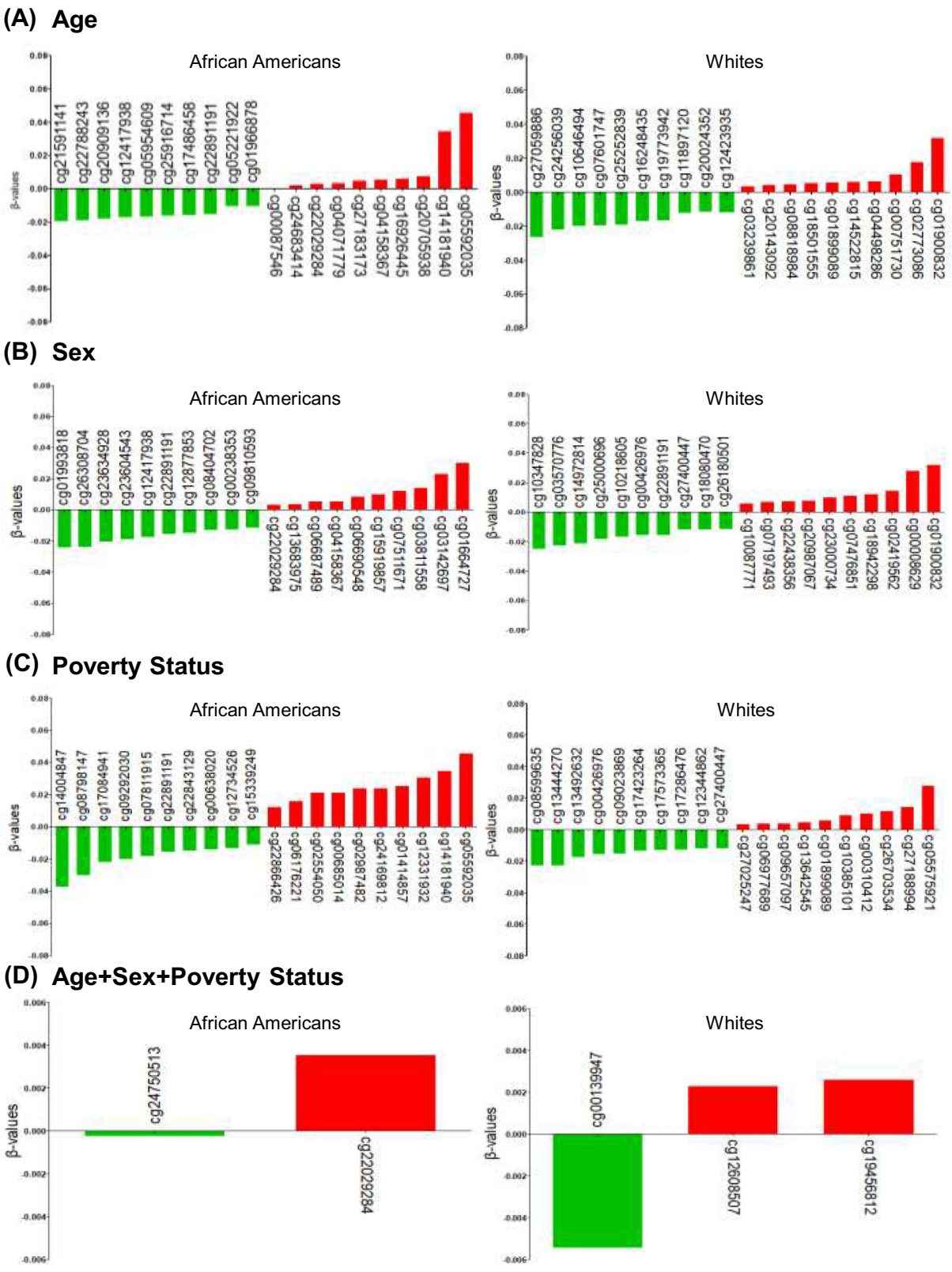


**Figure 1** Significant differentially DNA-methylated CpG sites for lifetime discrimination among African American and White participants with demographic variables: (A) age, (B) sex, (C) poverty status, and (D) age, sex, and poverty status. Green bars represent CpG sites that are hypomethylated; red bars represent CpG sites that are hypermethylated. Panels (A)–(C) show the top 10 significantly hyper- and hypomethylated CpG sites; panel (D) shows all the significant hyper- and hypomethylated CpG sites.

**Table 1** Most significantly differentially methylated CpG sites associated with lifetime discrimination with age in HANDLS ($P$-value $< .05$).

| African Americans | | | |
|---|---|---|---|
| **Gene symbol** | **CpG site** | **$\beta$-value** | **Function** |
| *MAD1L1* | cg16393715 | −0.00092 | Polymorphisms are associated with schizophrenia susceptibility [68] |
| *CD300A* | cg14181940 | 0.03483 | Modulate immune cell functions [69] |
| *PTPRN2* | cg07783094 | −0.00858 | Associated with childhood obesity [70] |
| *RERE* | cg11072627 | −0.00043 | Role in neurodevelopmental disorder [71] |
| *ARHGAP26* | cg21591141 | −0.01976 | Polymorphisms are associated with Alzheimer's disease and cardiovascular disease [72] |
| *FAM160B1* | cg12417938 | −0.01737 | Associated with behavioral abnormalities [73] |
| *PRKAR1B* | cg25001831 | −0.00772 | Variants cause neurodevelopmental disorders [74] |
| *GFI1* | cg04158367 | 0.00583 | Role in the epigenetic regulation of acute myeloid leukemia [75] |
| *PRDM16* | cg00087546 | 0.00243 | Involved in age dependent cardiac hypertrophy, adverse remodeling, mitochondrial dysfunction, and heart failure [76] |
| *ICA1* | cg22313239 | −0.00382 | Variations are associated with type 1 diabetes [77] |
| | | Whites | |
| Gene symbol | CpG site | $\beta$-value | Function |
| *ARHGAP26* | cg19456812 | 0.00262 | Associated with, cancer, Alzheimer's disease, and cardiovascular disease [32, 72] |
| *CORO2B* | cg08290628 | −0.01148 | Role in diabetic nephropathy [78] |
| *PTPRN2* | cg11202265 | 0.00255 | Associated with childhood obesity [70] |
| *MCC* | cg02951292 | −0.00624 | Associated with the predisposition of colon cancer [79] |
| *RERE* | cg16958658 | 0.00216 | Role in neurodevelopmental disorder [71] |
| *C7orf50* | cg04194173 | −0.0095 | Role in type 2 diabetes [80] |
| *RPS6KA2* | cg20669159 | −0.01045 | Role in prostate cancer [81] |
| *POU6F2* | cg12423935 | −0.01181 | Role in cancers [82] |
| *SBF2* | cg27156515 | −0.01055 | Role in glioblastoma [83] |
| *PRKAR1B* | cg26461009 | −0.00591 | Variants cause neurodevelopmental disorders [74] |

significantly differentially methylated CpGs are listed in Table 2 (top panel).

There were 112 CpG sites significantly methylated with Ldisc among White participants in this analysis. The top 10 hypermethylated CpG sites in Fig. 1B second column (red bars) are associated with genes: *CDC42BPB*, *SBF2*, *PACS1*, *MFHAS1*, *CTBP2*, *NIFK-AS1*, *JPH2*, *ROD1*, and *ATP9A*. The top 10 hypomethylated CpG sites (green bars) are in the following genes: *RASIP1*, *TRAF1*, *MTMR2*, *PTPRN2*, *SHANK3*, *PTPRE*, and *CLYBL*. The most significantly differentially methylated CpGs are listed in Table 2 (bottom panel).

This poverty-adjusted analysis (Model 3) identified 28 significantly methylated CpG sites for Ldisc, including poverty status in the model. Among African American participants, the top 10 hypermethylated CpG sites showed in Fig. 1C (red bars) are associated with the following genes: *RUNX1*, *CD300A*, *AHNAK*, *MLLT1*, and *GPR146*. The top 10 hypomethylated CpG sites (green bars) are associated with the following genes: *MAD1L1*, *DTHD1*, *CAPN13*, *PTPRN2*, *TPK1*, *PTPRE*, and *ERICH1*. The most significantly differentially methylated CpGs are listed in Table 3 (top panel).

Among White participants, we found 141 significantly methylated CpG sites for Ldisc in the poverty-adjusted model. The top 10 significantly hypermethylated CpG sites shown in Fig. 1C-second column (red bars) are associated with the following genes: *SMG6*, *PARD6G*, *NEDD4L*, *BCL3*, *AHRR*, *PRKAR1B*, *SEMA7A*, and *PARD3*. The top 10 most hypomethylated CpGs (green bars) in this group are associated with these genes: *WWOX*, *LINC00578*, *PARD3*, *SHANK3*, *ARHGAP22*, *JPH2*, *PACS1*, *PTPRN2*, *CD8A*, and *CLYBL*. The most differentially methylated CpGs are listed in Table 3 (bottom panel).

The age-, sex-, and poverty status-adjusted model (Model 4) analysis among African American study participants identified one hypermethylated CpG site, cg22029284 (red bar), in the *PRDM16* gene and one significantly hypomethylated CpG site, cg24750513 (green bar), in the gene *BIN1* (Fig. 1D) and Table 4 (top panel). The analysis among White participants (Fig. 1D, second column) identified two significantly hypermethylated CpG sites cg12608507 and cg19456812 (red bars) and Table 4 (bottom panel). These CpG sites are in the genes *EEF1B2* and *ARHGAP26*, respectively. There was only one significantly hypomethylated CpG site cg00139947 (green bar), which is in the gene *TOP1MT*.

## Analysis of CpGs and candidate genes previously associated with PD

Previously published work by others has identified differentially methylated CpG sites and genes that are associated with PD and with various conditions associated with racial and ethnic health disparities, including blood pressure level, diabetes mellitus, inflammation, and renal function [22–26]. To further validate our findings, we examined whether these previously published differentially methylated genes associated with PD overlapped with genes and their respective CpG sites in our data set [16, 18] (Figs 2–4 and Table S2). This analysis was performed using age, sex, and poverty status as covariates separately in African American and White participants.

First, we identified CpG sites that were significantly methylated in our dataset that overlapped with the CpGs previously identified in the published literature as associated with PD. One CpG site, cg16393715 in the gene *MAD1L1*, that was previously reported to be

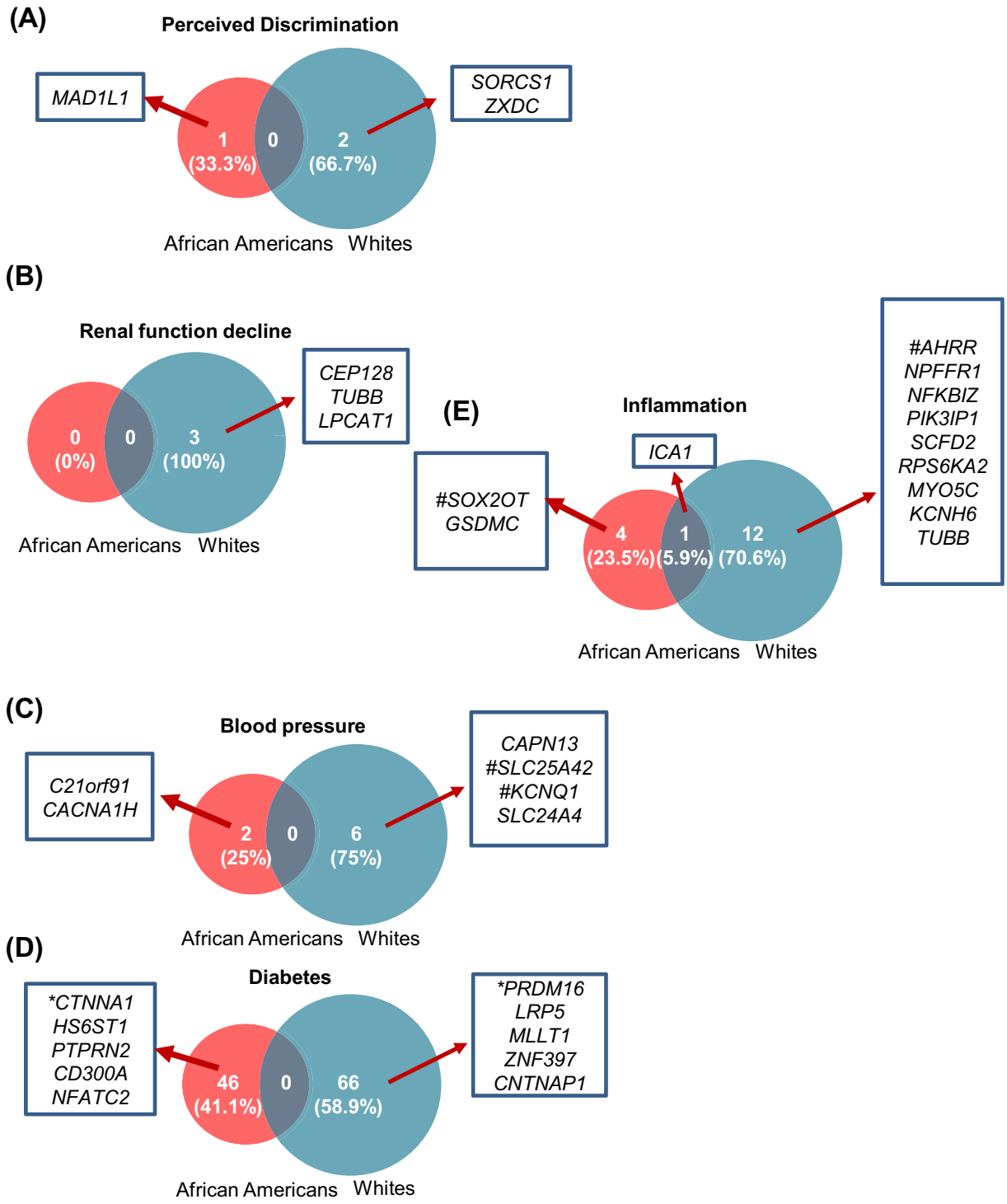


**Figure 2** Venn analysis identifying overlaps between genes significantly methylated with lifetime discrimination in HANDLS and previously reported to be significantly methylated with PD and conditions associated with health disparities with age: (A) PD—Venn diagram showing overlap between CpGs/genes differentially methylated in HANDLS and previously reported PD-related genes. (B) Renal function decline—Venn diagram showing overlap between genes differentially methylated in HANDLS with PD and those previously reported renal function decline-related genes. (C) Blood pressure—Venn diagram showing overlap between genes differentially methylated in HANDLS with PD and previously reported blood pressure-related genes. (D) Diabetes—Venn diagram showing overlap between genes differentially methylated in HANDLS with PD and previously reported diabetes mellitus-related genes. (E) Inflammation—Venn diagram showing overlap genes differentially methylated in HANDLS with PD and previously reported inflammation-related genes. ∗Only the top five methylated genes were represented. #Gene with more than one CpG site differentially methylated.

**Table 2** Most significantly differentially methylated CpG sites associated with lifetime discrimination associated with sex in HANDLS (*P*-value $< .05$).

| African Americans | | | |
|---|---|---|---|
| **Gene symbol** | **CpG site** | ***β*-value** | **Function** |
| *CORO2B* | cg12390780 | 0.00335 | Role in diabetic nephropathy [78] |
| *ERICH1* | cg11857858 | −0.0037 | DNA methylation patterns are associated with obesity [84] |
| *MAD1L1* | cg25259697 | −0.0089 | Polymorphisms are associated with schizophrenia susceptibility [68] |
| *PTPRN2* | cg26308704 | −0.02372 | Associated with childhood obesity [70] |
| *PARD3* | cg06832449 | −0.00292 | Role in cancer [85] |
| *NPR1* | cg07299819 | −0.00172 | Associated with renal function [86] |
| *SLC7A11* | cg06690548 | 0.00889 | Plays a key role in tumor growth [87] |
| *FAM160B1* | cg12417938 | −0.01737 | Associated with behavioral abnormalities [73] |
| *PRKAR1B* | cg22994830 | −0.01086 | Variants cause neurodevelopmental disorders [74] |
| *GFI1* | cg04158367 | 0.00583 | Role in the epigenetic regulation of acute myeloid leukemia [75] |
| Whites | | | |
| Gene symbol | CpG site | *β*-value | Function |
| *WWOX* | cg01256026 | −0.01122 | Loss of function in neurodevelopmental and neurodegenerative disorders [88] |
| *CORO2B* | cg08290628 | −0.01148 | Role in diabetic nephropathy [78] |
| *MCC* | cg15391499 | 0.00159 | Associated with the predisposition of colon cancer [79] |
| *MAD1L1* | cg10196995 | −0.01095 | Polymorphisms are associated with schizophrenia susceptibility [68] |
| *PTPRN2* | cg00369443 | −0.01032 | Associated with childhood obesity [70] |
| *RERE* | cg01162877 | −0.00435 | Role in neurodevelopmental disorder [71] |
| *PARD3* | cg27298509 | −0.00769 | Role in cancer [85] |
| *C7orf50* | cg26568662 | −0.00492 | Role in type 2 diabetes [80] |
| *ERICH1* | cg16040935 | −0.01123 | DNA methylation patterns are associated with obesity [84] |
| *RPS6KA2* | cg13906646 | −0.00441 | Role in prostate cancer [81] |

differentially methylated with PD was significantly associated with the lifetime discrimination instrument in the age-adjusted model among African American participants (Fig. 2 panel A, red circle). For sex and lifetime discrimination in African American participants, we found that CpG sites cg07485685, cg25259697, and cg05411165 were significantly methylated (Fig. 3 panel A, red circle). Two of these CpGs were in the gene *ABR*, and the other was in the gene *ABLIM2*. For poverty status and lifetime discrimination among African American participants, CpG sites cg12734526, cg14004847, cg03575939, cg09742952, and cg21089453 were significantly methylated (Fig. 4 panel A, red circle) and associated with genes *MAD1L1* and *TMEFF1*. There was more than one CpG site associated with the *MAD1L1* gene. Therefore, among African American participants, we reported overlap with CpG sites that have been previously associated with PD.

Next, we examined whether there was overlap of differentially methylated CpG sites previously reported with PD with Ldisc in White HANDLS participants. We found that the CpG sites cg08818984, cg07733851, cg03239861, cg04498286, cg11897120, cg18944144, and cg22070462 were significantly methylated with age (Fig. 2 panel A, blue circle). These CpG sites were associated with the two genes *SORCS1* and ZXDC. For sex, the analysis showed significant methylation at CpG sites cg01256026, cg09396019, cg10196995, cg23846046, cg00008629, cg02349373, cg12727138, cg18683606, and cg19247475 (Fig. 3 panel A, blue circle). These CpGs are associated with several genes displayed in the box adjacent to the blue circle. There were two CpGs associated with the *SRRT* gene. The analysis with poverty status revealed that CpG sites cg01256026, cg03943446, cg07300192, cg08599635, cg18353661, cg21998840, cg24297873, cg00219598, cg01805469, cg06502071, cg08293408, cg21942646, and cg22391718 were significantly methylated among White participants (Fig. 4 panel A, blue circle) and associated with six genes. One gene, *UGP2*, had more than one CpG site. Interestingly, the Venn diagram showed that these significantly differentially methylated CpG sites are race-specific with no significant overlap between African American and White participants for previously reported PD genes with age, sex, or poverty status (Fig. 2 panel A, Fig. 3 panel A, and Fig. 4 panel A).

## Analysis of candidate genes previously associated with renal function decline

Examining overlap between previous findings of differentially methylated genes and CpGs with renal function decline [26] in HANDLS participants and lifetime discrimination showed more differentially methylated CpG sites among White compared to African American participants. Among White participants, we identified three CpG sites that remained significantly associated with the lifetime discrimination instrument after adjustment for age (Fig. 2 panel B, blue circle). There were no significant CpG sites identified among African American participants (Fig. 2 panel B, red circle). With sex (Fig. 3 panel B, red circle), among African American participants, we found one CpG site differentially methylated in the gene *UCP2*. In White participants, we found five CpG sites associated with the four genes listed in the box adjacent to the blue circle (Fig. 3 panel B). The gene *LPCAT1* had more than CpG site. With poverty status, four CpG sites were significantly methylated among the White participants (Fig. 4 panel B, blue circle). For the African American participants, with poverty status, there was no significantly methylated CpG site (Fig. 4B, red circle).

**Table 3** Most significantly differentially methylated CpG sites associated with lifetime discrimination associated with poverty status in HANDLS (*P*-value < .05).

| **African Americans** | | | |
|---|---|---|---|
| **Gene symbol** | **CpG site** | ***β*-value** | **Function** |
| *AHNAK* | cg00685014 | 0.02155 | Associated with poor outcome of pancreatic ductal adenocarcinoma prognosis [89] |
| *MAD1L1* | cg14004847 | −0.03723 | Polymorphisms are associated with schizophrenia susceptibility [68] |
| *CD300A* | cg05592035 | 0.04584 | Modulate immune cell functions [69] |
| *PTPRN2* | cg00638020 | −0.01412 | Associated with childhood obesity [70] |
| *ERICH1* | cg22843129 | −0.01487 | DNA methylation patterns are associated with obesity [84] |
| *GPR146* | cg01414857 | 0.02571 | Associated with altered DNA methylation patterns among the African American patients with colorectal neoplasia [90] |
| *POU6F2* | cg19704451 | −0.00657 | Role in cancers [82] |
| *TPK1* | cg07811915 | −0.01813 | Predictive marker for the anti-tumor effects in gastric cancer [91] |
| *NOP58* | cg17930737 | 0.00667 | Prognostic marker in hepatocellular carcinoma [92] |
| *DTHD1* | cg08798147 | −0.0303 | Polymorphisms confer risk for hepatocellular carcinoma [92, 93] |
| | | Whites | |
| Gene symbol | CpG site | *β*-value | Function |
| *WWOX* | cg01256026 | −0.01122 | Loss of function in neurodevelopmental and neurodegenerative disorders [88] |
| *SLC12A7* | cg08293408 | −0.00551 | Role in adrenocortical carcinoma [94] |
| *MAD1L1* | cg21998840 | −0.00454 | Polymorphisms are associated with schizophrenia susceptibility [68] |
| *PTPRN2* | cg20030024 | −0.01075 | Associated with childhood obesity [70] |
| *RERE* | cg08548328 | −0.00682 | Role in neurodevelopmental disorder [71] |
| *SORCS2* | cg02447115 | −0.00968 | Required for social memory [95] |
| *SCARB1* | cg23460943 | −0.01011 | Inherited variants cause early-onset coronary artery disease [96] |
| *PARD3* | cg27188994 | 0.01468 | Role in cancer [85] |
| *C7orf50* | cg01778643 | −0.0085 | Role in type 2 diabetes [80] |
| *ERICH1* | cg21740055 | −0.00896 | DNA methylation patterns are associated with obesity [84] |

**Table 4** Significantly differentially methylated CpG sites associated with lifetime discrimination with age, sex, and poverty status in HANDLS (*P*-value < .05).

| **African Americans** | | | |
|---|---|---|---|
| **Gene symbol** | **CpG site** | ***β*-value** | **Function** |
| *BIN1* | cg24750513 | −0.000261857 | Susceptibility gene for Alzheimer's disease [28] |
| *PRDM16* | cg22029284 | 0.003540734 | Involved in age dependent cardiac hypertrophy, adverse remodeling, mitochondrial dysfunction, and heart failure [76] |
| | | Whites | |
| Gene symbol | CpG site | *β*-value | Function |
| *ARHGAP26* | cg19456812 | 0.002621218 | Associated with cancer, Alzheimer's disease, and cardiovascular disease [32, 72] |
| *EEF1B2* | cg12608507 | 0.002309914 | Role in cancer, neurodevelopmental disorders [97, 98] |
| *TOP1MT* | cg00139947 | −0.005440972 | Role in cancer, early-onset Parkinson disease [33, 99] |

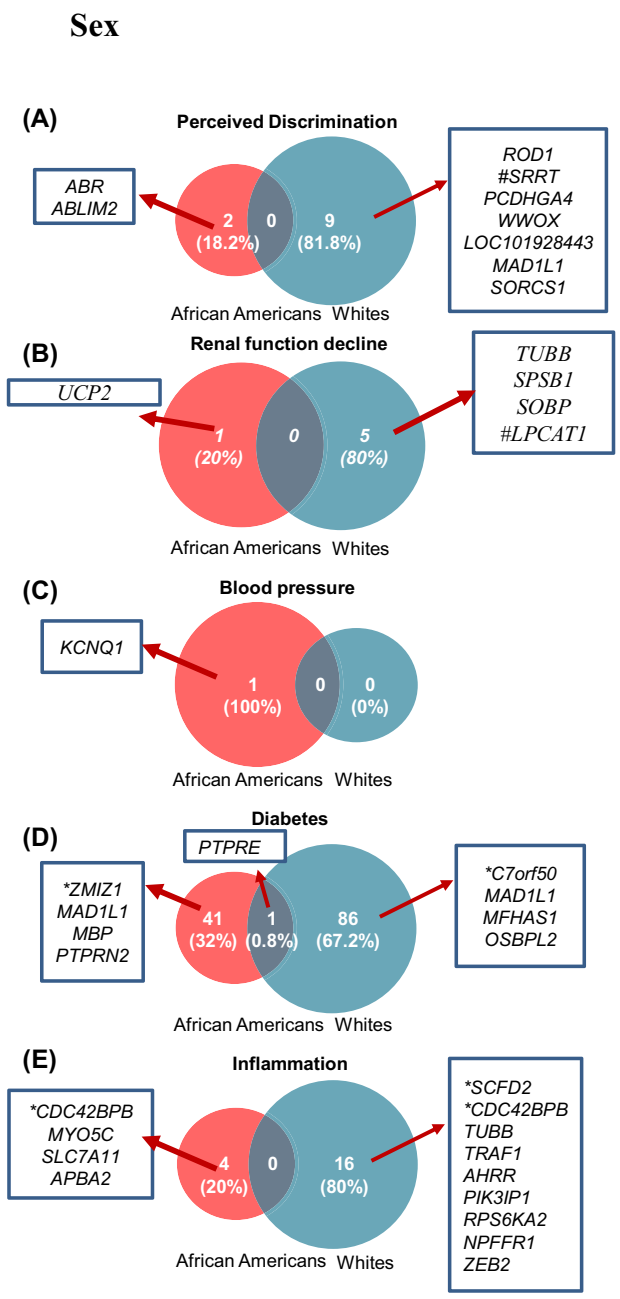


**Figure 3** Venn analysis identifying overlaps between genes significantly methylated with lifetime discrimination in HANDLS and previously reported significantly methylated with PD and conditions associated with health disparities associated with sex: (A) PD—Venn diagram showing the overlap between CpGs/genes differentially methylated in HANDLS and previously reported discrimination-related genes. (B) Renal function decline—Venn diagram showing CpGs differentially methylated with discrimination in HANDLS and previously reported for renal functional decline. (C) Blood pressure—Venn diagram showing the overlap between CpGs/genes differentially methylated with discrimination in HANDLS and previously reported blood pressure-related genes. (D) Diabetes—Venn diagram showing the overlap between CpGs/genes differentially methylated in HANDLS with discrimination and previously reported diabetes mellitus-related genes. (E) Inflammation—Venn diagram showing overlap CpGs/genes differentially methylated in HANDLS with discrimination and previously reported inflammation-related genes. ∗Only the top five methylated genes represented. #Gene with more than one CpG site differentially methylated.

## Analysis of candidate genes previously associated with blood pressure

Using our candidate gene approach for blood pressure-related genes [22, 24], we examined the overlap in our data set with blood pressure-related genes. We found that among African American participants, CpG sites cg05531134 and cg26915870 were significantly methylated with age and lifetime discrimination (Fig. 2C, red circle). The genes associated with these CpGs are associated with the genes listed in the adjacent box. Among White participants, we found significant methylation at the CpG sites cg02079326, cg04661001, cg13993469, cg18729298, cg23484461, and cg27491887 with age (Fig. 2C, blue circle). These CpGs are associated with the four genes listed in the adjacent box. Two of these genes were associated with more than one CpG site. There was only one CpG site significantly methylated with sex, cg06914593, in African American participants (Fig. 3C, red circle). The associated gene is listed in the adjacent box. There were no CpGs among White participants. Both cg07354679 and cg17084941 were significantly methylated with poverty status among African American study participants (Fig. 4C, red circle). Three CpG sites were significantly methylated with poverty status among White participants, cg04106390, cg14826184, and cg16663063 (Fig. 4C, blue circle). The associated genes are listed in the adjacent boxes. One gene *CACNA1H*, calcium voltage-gated channel subunit alpha1H, is significantly differentially methylated in both African American and White participants with blood pressure and poverty status. However, the differentially methylated CpGs do not overlap between African American and White participants.

## Analysis of candidate genes previously associated with diabetes mellitus

Similarly, using our lifetime discrimination data, we performed a gene candidate approach for previously reported diabetes-related genes [27]. We identified several overlaps between CpG sites associated with discrimination and previously published diabetes-related genes and CpG sites. This analysis among the African American participants revealed 46 significantly methylated CpG sites associated with age (Fig. 2D, red circle). The associated genes are listed in the adjacent box. There were 66 significantly methylated CpG sites associated with age among White participants (Fig. 2D, blue circle) with age. The associated genes are listed in the adjacent box. We identified 42 significantly methylated CpG sites associated with sex (Fig. 3D) in African American participants and 87 CpG sites associated with sex (Fig. 3D) in White participants. There was one CpG site that overlapped between African American and White participants (Fig. 3D). It is associated with the gene *PTPRE*, protein tyrosine phosphatase receptor type E, which is involved in signaling molecules that regulate cell growth, differentiation, mitosis, and cellular transformation.

In this analysis, there were 22 significantly methylated CpG sites for diabetes-related genes that were also found to be associated with poverty status among African Americans (Fig. 4D, red circle). Among White participants, we identified 115 CpG sites associated with poverty status that overlapped with CpG sites in diabetes-related genes.

The age-, sex-, and poverty status-adjusted analyses for lifetime discrimination using CpG sites and genes associated with diabetes mellitus identified only two significantly methylated CpG sites, cg22029284 (*PRDM16*) and cg24750513 (*BIN1*) among African American study

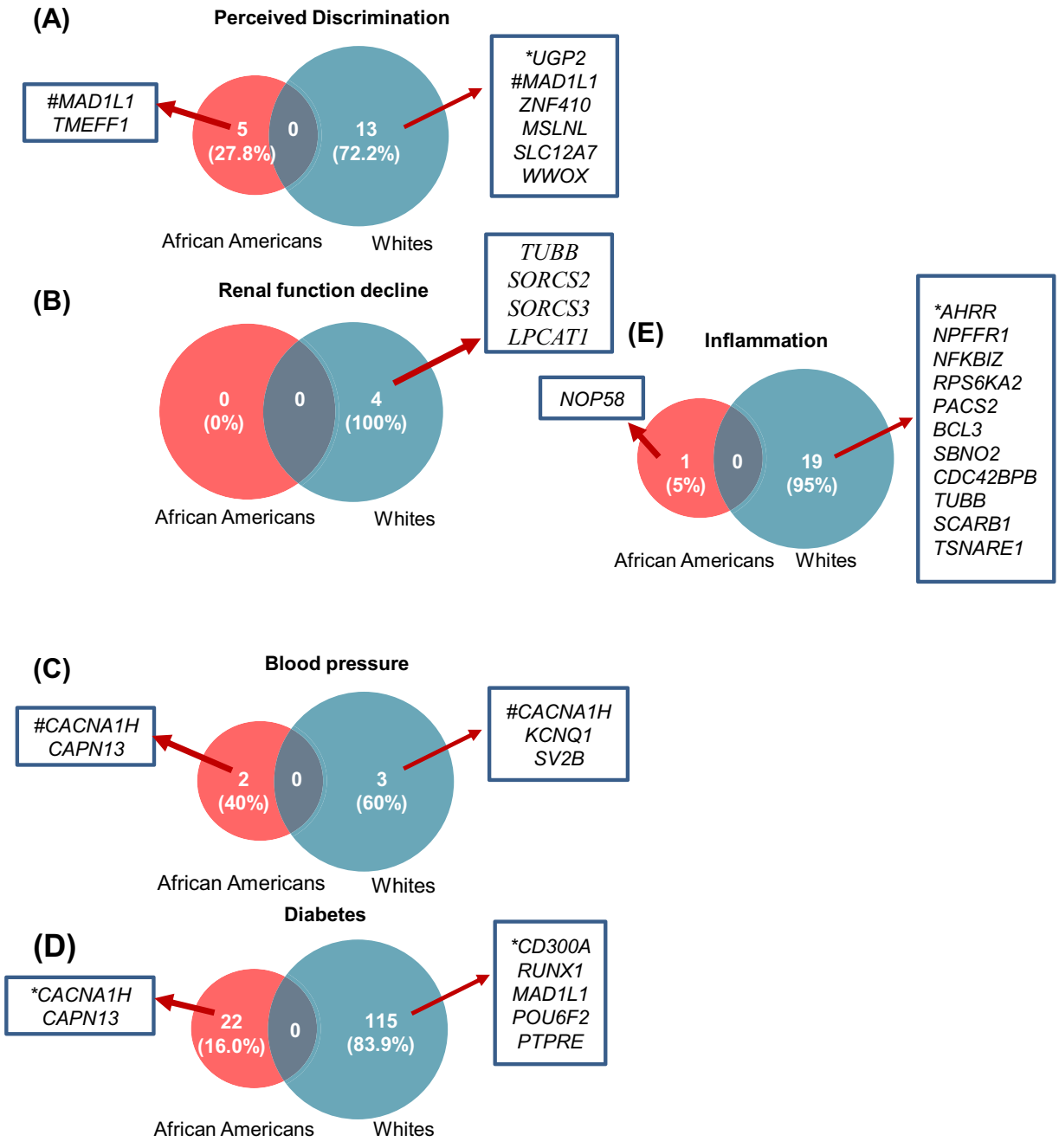


**Figure 4** Venn analysis identifying overlaps between CpG sites/genes significantly methylated with lifetime discrimination in HANDLS and previously reported significantly methylated with PD and conditions associated with health disparities associated with poverty status: (A) PD—Venn diagram showing the overlap between CpGs/genes differentially methylated in HANDLS and previously reported PD-related genes. (B) Renal function decline—Venn diagram showing CpGs differentially methylated with discrimination in HANDLS and previously reported for renal function decline. (C) Blood pressure—Venn diagram showing the overlap between CpGs/genes differentially methylated in HANDLS with discrimination and previously reported blood pressure-related genes. (D) Diabetes—Venn diagram showing the overlap between CpGs/genes differentially methylated in HANDLS with discrimination and previously reported diabetes mellitus-related genes. (E) Inflammation—Venn diagram showing overlap CpGs/genes differentially methylated in HANDLS with PD and previously reported inflammation-related genes. ⁎Only the top five methylated genes were represented. [#]Gene with more than one CpG site.

participants that were also differentially methylated with diabetes mellitus. There were only three significantly methylated CpG sites, cg00139947 (*TOP1MT*), cg12608507 (*EEF1B2*, *SNORA41*, *SNORD51*, *NDUFS1*), and cg19456812 (*ARHGAP26*) associated with m among White participants (Table S28H). We did not identify CpGs that overlapped with age + sex + poverty status for the other diseases or conditions examined in our study.

## Analysis of candidate genes previously associated with chronic low-grade inflammation

When we examined previously reported candidate genes associated with inflammation [25], we identified among African American participants, five significantly methylated CpG sites associated with age and lifetime discrimination (Fig. 2E, red circle). There were 13 associated with age among White participants (Fig. 2E, blue circle); one of these CpGs overlapped with African American participants. This CpG is associated with the gene islet cell autoantigen 1, which is associated with insulin-dependent diabetes and autoimmune disease. We noted four significantly associated with sex among African American participants (Fig. 3E, red circle). We found 16 significantly methylated CpGs associated with sex among White participants (Fig. 3E, blue circle), but none of these overlapped with those found among African American participants. There was only one CpG site cg17930737 associated with poverty status for African American participants (Fig. 4E, red circle). Among White participants, we found 19 significantly methylated CpG sites, but none of these overlapped with the CpG site among African American participants (Fig. 4E, blue circle). Overall, our results in the HANDLS cohort identified a significant number of CpG sites that were differentially methylated with PD as measured by Ldisc that overlap with differentially CpG sites and genes suspected to play a role in conditions associated with health disparities.

## Functional analysis of the CpG sites significantly methylated with PD as measured by Ldisc

We performed Ingenuity Pathway Analysis (IPA) to examine which molecular and cellular pathways may be influenced by the CpG methylation patterns associated with PD with age, sex, poverty status, age + sex, and age + sex + poverty status. We imported the genes annotated to the significantly differentially methylated CpG sites into IPA for functional enrichment and pathway analysis. With age and lifetime discrimination, among African American participants, the functional analysis revealed that the white adipose tissue browning pathway was activated (Fig. 5A). This was related to the differential methylation found in the *BDNF*, *CACNA1H*, *PRDM16*,and *PRKAR1B* genes among African Americans with age (Fig. 5A). The IPA analysis revealed that for White participants, for CpG sites associated with PD with age, the opioid signaling pathway was activated and significantly enriched for the genes *FGR*, *POMC*, *RPS6KA2*, and *PRKAR1B* (Fig. 5B).

Results from the functional analysis for the CpG sites associated with PD among White participants with poverty status revealed that netrin signaling, opioid signaling, and calcium signaling pathways were the top pathways and that there was a significant enriched for the following genes: *ABLIM2*, *CACNA1H*, *NFATC1*, *NFATC2*, *PRKAR1B*, *AP2A2*, *CACNA1H*, *POMC*, *PRKAR1B*, *RPS6KA2*, *CACNA1H*, *NFATC1*, *NFATC2*, and *PRKAR1B* (Fig. 5C). The analyses for sex, age + sex, and age + sex + poverty status revealed no significant pathways among African American or White participants.

## Identification of differentially methylated CpGs associated with other forms of PD and age, race, sex, and poverty status

The age-adjusted analyses revealed 93 CpG sites were significant for Sdisc (Fig. S1 panel A and Table S3), 6 CpG sites were significant for Ldisc with age (Fig. S1 panel B and Table S4), 4 CpG sites were significant for Gdisc (Fig. S1 panel C, Table S5), and 261 CpG sites were significant for Rdisc (Fig. S1 panel D, Table S6) and no significant CpG sites for Edisc (Fig. S1 panel E) or Cdisc (Fig. S1 panel F). No significant CpG sites were found for any of the discrimination scales in race-adjusted analyses (Fig. S2 panels A–F).

The sex-adjusted analyses revealed 84 CpG sites significant for Sdisc (Fig. S3 panel A, Table S7), 7 CpG sites for Ldisc (Fig. S3 panel B, Table S8), 5 CpG sites for Gdisc (Fig. S3 panel C, Table S9), and 283 CpG sites for Rdisc (Fig. S3 panel D, Table S10), but no significant CpG sites for Edisc (Fig. S3 panel E) and Cdisc (Fig. S3 panel F).

The poverty-adjusted analyses revealed 87 CpG sites significant for Sdisc (Fig. S4 panel A, Table S11), 14 CpG sites for Ldisc (Fig. S4 panel B, Table S12), 5 CpG sites for Gdisc (Fig. S4 panel C, Table S13), and 327 CpG sites for Rdisc (Fig. S4 panel D, Table S14), but no significant CpG sites for Edisc (Fig. S4 panel E) or Cdisc (Fig. S4 panel F).

Results from the multivariable linear regression models adjusted for both age and sex showed that 97 CpG sites were significant for Sdisc (Fig. S5A, Table S15), 6 CpG sites were significant for Ldisc (Fig. S5 panel B, Table S16), 5 CpG sites were significant for Gdisc (Fig. S5 panel C, Table S17), and 283 CpG sites were significant for Rdisc (Fig. S5 panel D, Table S18), but no CpG sites for Edisc (Fig. S5 panel E) and Cdisc (Fig. S5 panel F).

The age, sex, and poverty status analyses identified 104 CpG sites significant for Sdisc (Fig. S6 panel A, Table S19), 20 CpG sites for Ldisc (Fig. S6 panel B, Table S20), 5 CpG sites for Gdisc (Fig. S6 panel C, Table S21), and 361 CpG sites for Rdisc (Fig. S6 panel D, Table S22), but no CpG sites significant for the Edisc (Fig. S6 panel E) and Cdisc (Fig. S6 panel F).

We examined the overlap of differentially methylated CpG sites that were significant in the different discrimination scales. This analysis showed that there was no overlap in CpG sites between discrimination scales in our age, sex, age + sex, and age + sex + poverty status analyses (Fig. S7 panels A, B, D, and E). We found that one CpG site cg04118610, located in the Adhesion G Protein-Coupled Receptor L3 (*LPHN3*) gene, was significant in all the discrimination scales for the poverty-adjusted model (Fig. S7 panel C).

## Differentially methylated positions associated with lifetime and racial discrimination with age, sex, and poverty status

Next, we used the *dmpFinder* function for the two discrimination scales, Ldisc and Rdisc, to identify the differentially methylated positions (DMPs) associated with each scale. This analysis revealed a significant number of CpGs associated with lifetime and racial discrimination, with age + sex + poverty status at $P < .05$. To select the most robustly associated DMPs, we used a $P < .01$ cut-off. The more stringent DMP analysis demonstrated that among the 16 771 DMPs that were significant at a $P < .01$ for Ldisc, 4356 (25.9%) CpG sites were hypermethylated. The top hypermethylated CpGs based on $\beta$-values and associated genes included *TMEM154*-Transmembrane Protein 154 (cg16203592),

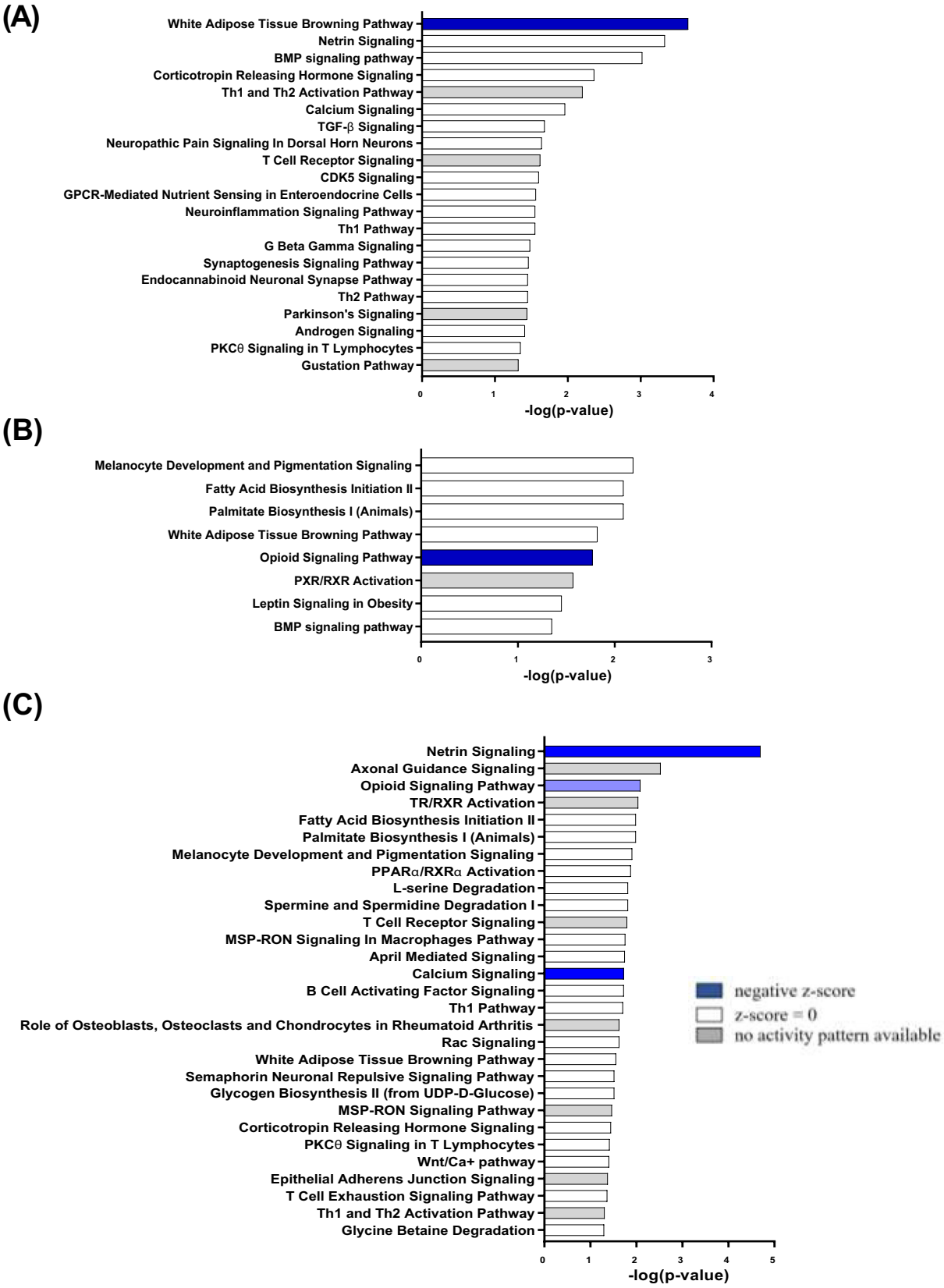


**Figure 5** IPA of significantly methylated CpGs associated with lifetime discrimination among African American and White participants. (A) Top canonical pathways for the age-associated CpG sites associated with PD in African American participants. (B) Top canonical pathways for the age-associated CpG sites associated with PD in White participants. (C) Top canonical pathways for the poverty status-associated CpG sites associated with PD in White participants. Blue bars represent the pathways that are inactivated ($Z$-score $<-2$). The $P$-value for each pathway is represented by the bar and is expressed as a $-\log$ ($P$-value).

*EIF3A*-Eukaryotic Translation Initiation Factor 3 subunit A (cg24623109), IQ motif containing-*IQCK* (cg03615426), and Copper Chaperone for Superoxide Dismutase *CCS* (cg24851651). In addition, there were 12 415 (74.0%) CpG sites that were hypomethylated. The top hypomethylated genes were *LOC101927924*-long intergenic non-protein coding RNA 1856 (cg07929412), *SLN*-Sarcolipin (cg20221740), *GPR1-AS*-Chemerin chemokine-like receptor 2 (cg22444562), *TMEM63B*-Transmembrane protein 63B (cg25069157), *LPHN3* Adhesion G protein-coupled receptor L3 (cg04118610), *OR2T5*-Olfactory Receptor family 2 subfamily T member 5 (cg27191320), *WWOX*-WW domain containing oxidoreductase (cg02171206), *PAWR*-Pro-apoptotic WT1 regulator (cg11258982), and *TMEM9B*-Transmembrane Protein 9 domain family member B (cg15570860).

For Rdisc, we found that among the 33 990 DMPs that were significant, 15 046 (44.2%) CpG sites were hypermethylated. The most hypermethylated genes were *TMEM154* (cg16203592), *LOC101928708* (cg03146160), *EIF3A* (cg24623109), *CORO2B*-coronin, actin-binding protein, 2B (cg15917410), and *IQCK* (cg03615426). There were 18 944 (55.7%) hypomethylated CpG sites. The most hypomethylated genes included *SLN* (cg20221740), *TMEM9B* (cg15570860), *OR2T5* (cg27191320), *WWOX* (cg02171206), and *PAWR* (cg11258982).

### Gene network analysis regulatory effects

To better understand the regulatory effects of the pathways identified in our IPA analysis, we performed gene network analysis. We focused on the genes that were significantly enriched in the pathway analysis at a *P*-value < .05 (Fig. 5A–C). For the white adipose tissue browning pathway, we focused on *BDNF* (brain-derived neurotrophic factor), *CACNA1H* (calcium voltage-gated channel subunit alpha1H), *PRDM16 (*PR/SET domain 16), and *PRKAR1B* (protein kinase cAMP-dependent type I regulatory subunit beta) because they were differentially methylated. Our results showed that for the age-associated Ldisc CpG sites in African American participants, downregulation of the genes *BDNF* (Fig. 6A), *CACNA1H* (Fig. 6B), and *PRDM16* (Fig. 6C) was predicted to activate nitric oxide. Although the *PRKAR1B* gene was differentially methylated with age in African American participants, it did not predict the activation of any gene or molecule in the white adipose tissue browning pathway.

With age, the differential methylation of the Pro-opiomelanocortin (*POMC*) gene (Fig. 6D) was associated with activation of the opioid signaling pathway in White participants. With poverty status among White participants, the opioid signaling pathway was enriched for the following genes: FGR-proto-oncogene (*FGR*), ribosomal protein S6 kinase A2(*RPS6KA2*), adaptor-related protein complex 2 subunit alpha 2 (*AP2A2*), *PRKAR1B*, and *CACNA1H* (Fig. S8). Downregulation of the genes *FGR* (Fig. S8A) and *RPS6KA2* (Fig. S8B) was predicted to activate the genes BCL2-associated agonist of cell death (*BAD*), glycogen synthase 3 beta (*GSK3B*), ETS transcription factor ELK1 (*ELK1*), and AKT serine/threonine kinase 1 (*AKT1*). We found that downregulation of the gene *CACNA1H* (Fig. S8E) was predicted to activate adenosine triphosphate. Genes *AP2A2* (Fig. S8C) and *PRKAR1B* (Fig. S8D) on the other hand did not predict the activation of any gene or molecule in the opioid signaling pathway.

Our results showed that for the poverty status-associated Ldisc CpG sites in White participants, downregulation of the genes *NFATC1* (Fig. S9A) and *NFATC2* (Fig. S9C) was predicted to activate adenosine triphosphate and *MAPK3* (mitogen-activated protein kinase 3) gene and to inhibit the genes *PPP3R1* (protein phosphatase 3 regulatory subunit B, alpha), *RCAN1* (regulator of calcineurin 1), *MYH1* (myosin heavy chain 1), *HDAC1* (histone deacetylase 1), *NFATC3* (nuclear factor of activated T cells 3), and *MEF2D* (myocyte enhancer factor 2D) in the calcium signaling pathway. For the netrin signaling pathway, our results showed that downregulation of the genes *NFATC1* (Fig. S9B) and *NFATC2* (Fig. S9D) did not predict the activation of any gene or molecule that inhibited the genes *PPP3R1* and *NFATC3*.

Overall, our results demonstrate that Ldisc adjusted for age and poverty is associated with white adipose tissue browning, opioid signaling, netrin, and calcium signaling pathways through differential methylation of pathway-enriched genes. Psychosocial stress may have a role in important signaling pathways through differential DNAm in both African American and White adults.

## Discussion

Our data support the idea that differential DNAm is a relevant biological pathway through which psychosocial stress "gets under the skin." We identified novel, significantly differentially methylated CpGs and DMPs associated with a psychosocial stressor, PD, among African American and White adults. Many CpGs identified are involved in pathways that play fundamental roles in various chronic disease health disparities. Using our data set, we identified overlap with previously reported CpGs that were differentially methylated with exposure to PD or the presence of diseases and conditions associated with health disparities. This suggests that psychosocial stress as a toxic exposure may influence DNAm of CpGs that play roles in susceptibility to chronic disease. Functional and regulatory gene network analysis of significantly differentially methylated CpG sites with PD identified three important pathways: the white adipose tissue browning, the opioid signaling, and the calcium signaling pathways. Gene network analysis identified that PD and age were associated with white adipose tissue browning in African American participants, and PD and poverty were associated with the opioid signaling pathway in White participants. These network analyses also identified the calcium signaling pathway among White participants living in poverty and reporting perceived psychosocial stress. The identification of these pathways brings to the forefront the importance of stress in the activation of molecular signaling mechanisms that influence health and disease.

The race-stratified EWAS analysis for Ldisc demonstrated that these variables are significantly associated with DNAm and revealed several novel genes and CpG sites associated with PD. Many of these genes as referenced in Tables 1–4 have functions related to neurodegenerative diseases, including Alzheimer's disease, metabolic diseases, including diabetes mellitus types 1 and 2 and obesity, cancer, and neurodevelopmental disorders. The CpGs reported in Tables 1–4 are nominally significant findings ($P < .05$) and should be considered exploratory. The primary conclusions of the study are based on analyses that survived multiple-testing correction. The age-, sex-, and poverty-adjusted models were included primarily as sensitivity analyses to evaluate the stability of psychosocial stress-associated methylation signals under different covariate adjustments and to explore potential pathways through which social and demographic factors may influence these associations. Our primary interpretation focuses on the

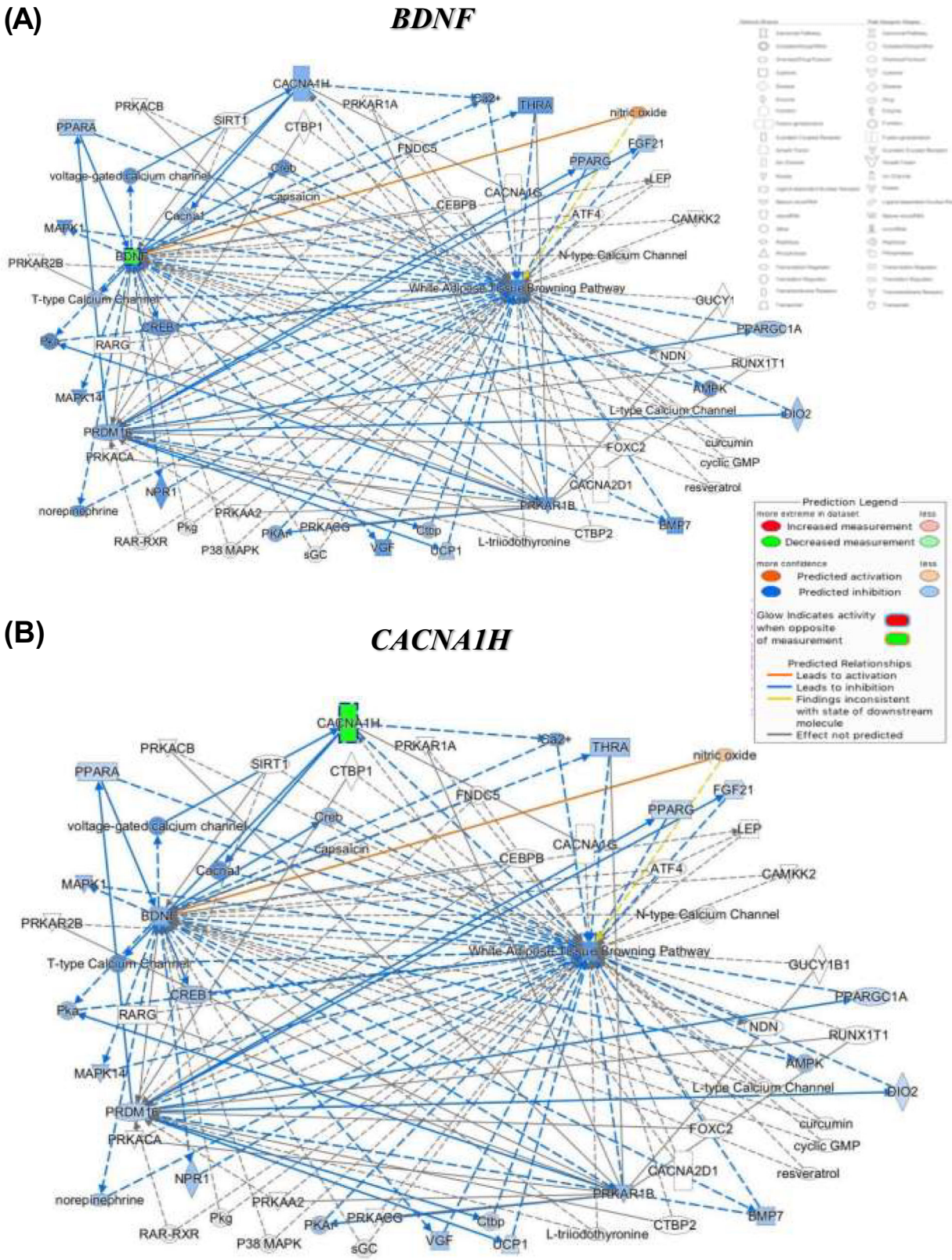


**Figure 6** Gene network analysis showing the regulatory effects in the white adipose tissue browning and opioid signaling pathways: (A) *BDNF*,(B) *CACNA1H*, and (C) *PRDM16* genes in the white adipose tissue browning pathway among African American participants and (D) *POMC* in the opioid signaling pathway among White participants. The relationship among the genes is represented by solid lines representing direct associations and dotted lines representing indirect associations. The darker shaded shapes indicate a higher predicted inhibition, while a lighter shaded shape indicates a lower predicted inhibition.

**(C)** ***PRDM16***

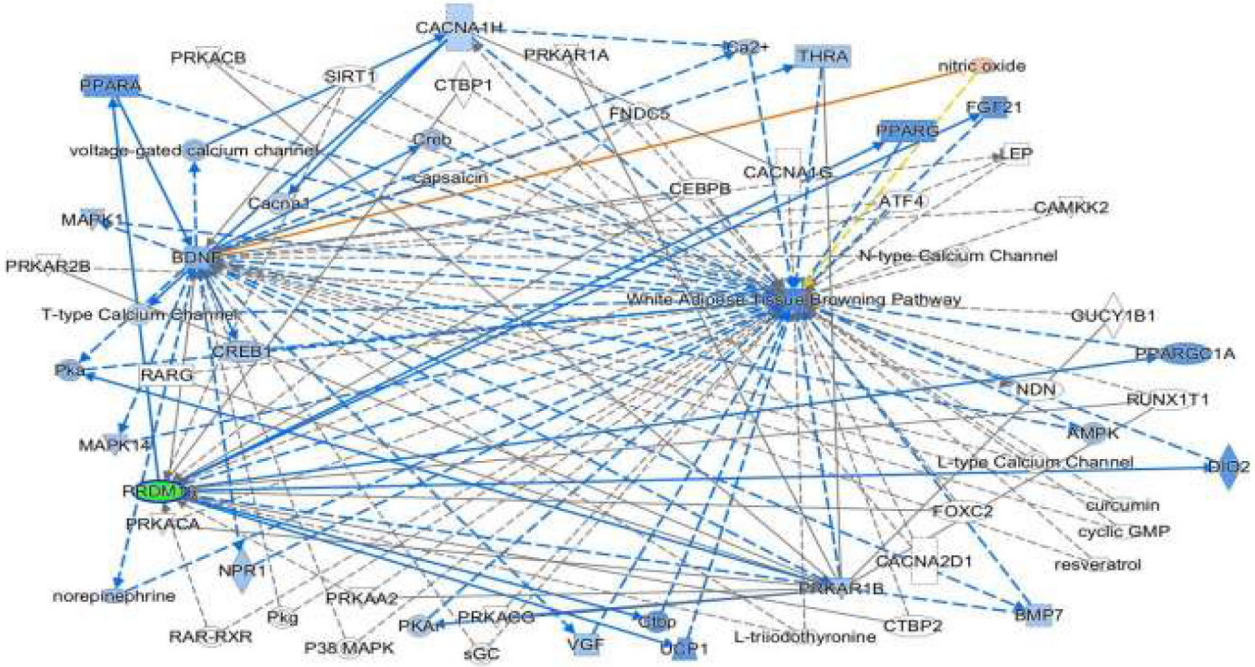


**(D)** ***POMC***

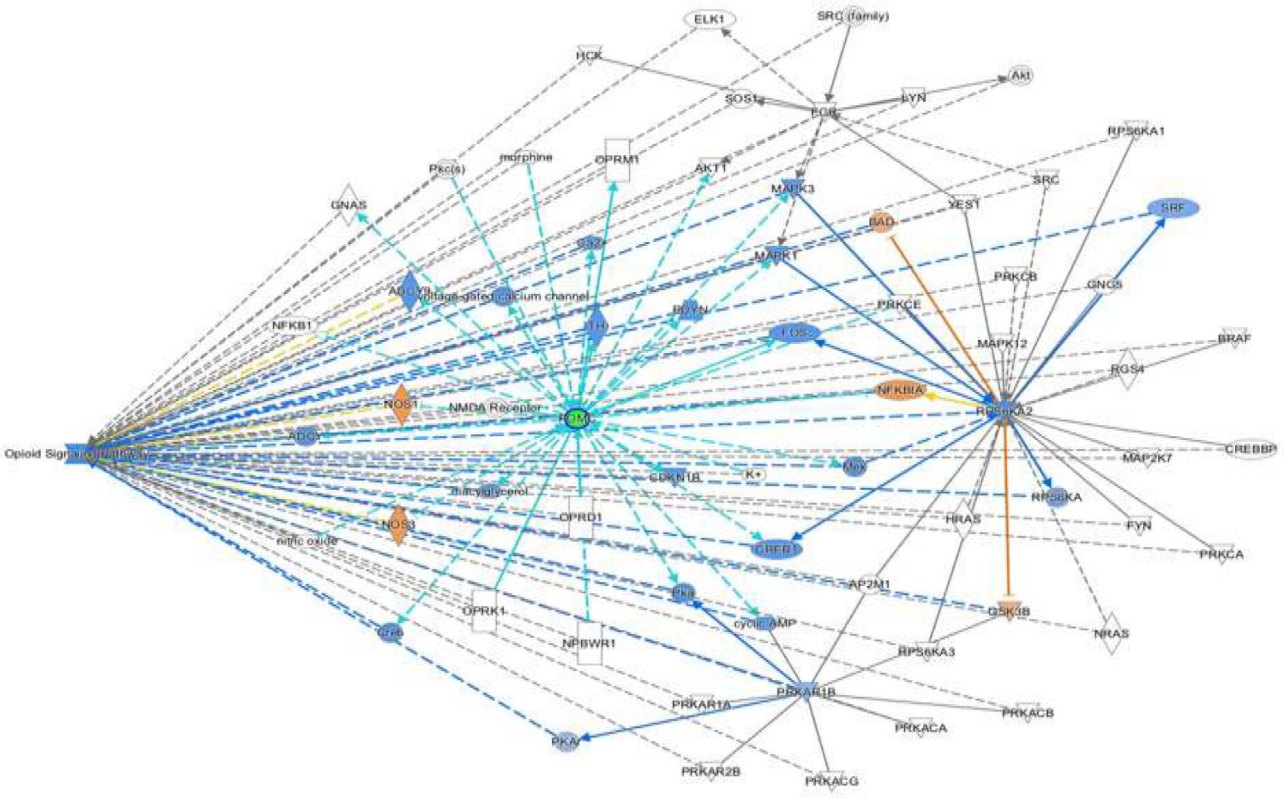


**Figure 6** (Continued).

fully adjusted model, which provides the most conservative assessment of the relationship between perceived stress and DNAm. Findings from partially adjusted models should therefore be considered exploratory and hypothesis-generating pending validation in independent cohorts. The significantly differentially methylated CpG sites associated with lifetime discrimination and age + sex + poverty status differed between African American and White participants. In African American participants, the differentially methylated CpG site (cg24750513) is associated with the *BIN1* gene, which produces the Bridging Integrator 1 protein. It is an important susceptibility gene for late-onset Alzheimer's disease second only to *APOE4* [28]. *BIN1* may modulate APP metabolism and synaptic transmission as well as influence Tau protein function and neurotoxicity. In our study, the CpG within *BIN1* was hypomethylated. It is interesting to note that hypomethylation of the *BIN1* promoter was associated with preclinical AD [29]. Given the significant disproportionate burden of dementia among African Americans, this finding may deserve further investigation. The other differentially methylated CpG among African American participants is in the *PRDM16* gene, which is involved in several molecular functions, including DNA-binding transcription activator activity and histone methyltransferase activity. It is also important in brown fat cell differentiation, energy homeostasis, as well as glucose and lipid metabolism (for review, see [30]). The differential methylation of these CpGs within these genes suggests that the pathway through which discrimination is transduced as a risk factor for obesity and cognitive decline involves the epigenetic alteration, DNAm, highlighting the importance of the epigenome in health disparities [5, 31].

Among White participants, three CpG sites were differentially methylated in the age + sex + poverty status adjusted analysis. These CpGs are in the following genes: RhoA GTPase-activating protein 26 (*ARHGAP26*), eukaryotic translation elongation factor 1$\beta$ 2 (*EEF1B2*), and DNA topoisomerase l mitochondrial (*TOP1MT*). *ARHGAP26* is involved in tumorigenesis as well as tumor promotion and invasion for selected cancers and as a biomarker of overall survival in others (for review, see [32]). *EEF1B2*, a subunit of eukaryotic translation elongation factor 1, plays a role in de novo protein synthesis. Mutations in *EEF1B2* lead to defects in the translational balance of protein synthesis and risk of neurodevelopmental disorders, including intellectual impairment and disability. *TOP1MT* is a human mitochondrial topoisomerase involved in DNA replication, chromatin remodeling, genomic stability, and DNA metabolism (for review, see [33]). In the EWAS models, among White participants, discrimination was associated with differential methylation of CpGs in genes that are associated with cancer, genomic stability, and neurodevelopmental disorders.

To validate our hypothesis that psychosocial stress influences health outcomes through differential DNAm of CpGs located in disease-relevant genes, we examined the overlap between our data and previously reported differentially methylated CpG sites and genes associated with discrimination stress, blood pressure, diabetes, inflammation, and renal function decline. Our study replicates many of the CpGs previously reported to be differentially methylated with discrimination [16, 18]. In addition, we found that CpGs differentially methylated with discrimination were also differentially methylated in chronic conditions that have disparate health outcomes for African Americans and other marginalized US populations in age-, sex-, and poverty status-adjusted analyses. For example, we identified several overlapping CpGs associated with discrimination in our study with those previously published. Our results demonstrated a significant number of CpG sites that were differentially methylated in these diseases with age, sex, and poverty status in both African American and White participants. Interestingly, the CpGs and genes differentially methylated with discrimination in our study have notable overlap with genes/CpGs that play important roles in diseases and conditions that are critical areas of health disparities, including diabetes mellitus, cardiovascular disease, cancer, depression, end stage renal disease. Additionally, these overlaps were also present among White participants suggesting that discrimination is a health risk for African American as well as White participants. The IPA analysis based on the significantly methylated CpGs linked to discrimination exposure among the African American and White participants revealed that, in the age-adjusted analysis among African American participants, the white adipose tissue browning pathway was activated, while among White participants, the opioid signaling pathway was activated. The poverty status-adjusted analysis revealed an over-representation of the netrin signaling, opioid signaling, and calcium signaling pathways among White participants. These molecular pathways play critical roles in human health and disease and are particularly relevant to health disparities. White adipose tissue, which stores food calorie energy as triglycerides, provides thermal insulation, and mechanical protection, is an endocrine organ that plays a role in immunity and inflammation among other physiologic processes (for review, see [34]). Netrin-1 plays a role in multiple physiologic processes playing important roles in cardiovascular and renal disease as well as cancer (for review, see [35]). In cardiovascular disease, Netrin-1 serves as a central modulator of atherosclerosis. Plasma levels of netrin are negatively correlated with plaque density and the extent of arterial wall inflammation [36, 37].

Calcium is a vital second messenger in cells that is critical in many aspects of cell physiology and function, including cellular differentiation and proliferation, metabolism, apoptosis, as well as gene expression. Calcium signaling plays a role in cancer, neurodegeneration, including Alzheimer's disease, cardiovascular disease, including hypertension and obesity, among other disease states. Opioid signaling functions in pain and pain modulation, and the neuroendocrine, reproductive, cardiovascular, and immune systems [38, 39, 40]. The netrin, opioid, and calcium signaling overrepresented in our results are known to be methylated in neurological disorders such as PTSD [41], opioid use disorder [42], and cancers, including breast cancer [43]. Furthermore, the regulatory effect analysis of these pathways in our study demonstrated that most of the methylated genes exert inhibitory effects in these pathways increasing the risk for unhealthy outcomes. For example, inhibition of the white adipose tissue browning pathway is associated with obesity and health risks associated with metabolic syndrome since the browning pathway reduces risk for obesity and metabolic syndrome [44, 45].

Our study has several notable strengths and limitations. Our cohort is diverse consisting of community-dwelling middle-aged African American and White participants. Our study considers the influence of potential covariates such as age, sex, and poverty status in discrimination studies. Our genome-wide DNAm analysis was performed using the latest version of EPIC compared to previous studies on discrimination, which used Illumina HumanMethylation450 array to quantify the methylation of CpG sites. Our study has limitations such as the non-inferring of causality between discrimination and DNAm. We have not included other social determinants of health that may influence the effects of discrimination on health outcomes nor have

we done any mediation analysis. Future work in this area should model coping as a covariate or mediator that might attenuate the association of discrimination as a stressor with epigenetic outcomes. In addition, this is a cross-sectional study. The sample size in our study is relatively small for an EWAS focusing on conducting race-stratified analyses. The DMP analysis was designed as a complementary exploratory approach to support interpretation of the EWAS findings. Because DNAm is strongly influenced by demographic and socioeconomic variables, careful adjustment for age, sex, race, and poverty status was necessary to minimize confounding. We therefore focused our primary interpretation on covariate-adjusted EWAS findings and considered DMP results primarily as supportive evidence. Furthermore, nominal significance thresholds are insufficient for genome-wide inference and should be interpreted as hypothesis-generating rather than definitive evidence of association. Further validation of the biological relevance of identified CpG sites with pathways of white adipose tissue browning and opioid signaling, and additional functional studies are necessary. Additionally, smoking status was not included in the primary EWAS models because smoking may act as both a potential confounder and a behavioral consequence of chronic psychosocial stress. Adjusting for smoking could therefore remove part of the biological signal through which psychosocial stress affects health.

## Conclusions

The main findings of this study are that perceived psychosocial stress is linked to consistent patterns of DNAm involving biological pathways related to immune function, metabolism, calcium signaling, and stress-responsive molecular networks. Although individual CpG sites varied across adjustment models and racial groups, several common themes appeared. First, only a small number of CpGs remained significant after full adjustment, indicating that many observed associations may be influenced by demographic and socioeconomic factors. Second, most psychosocial stress-related methylation signatures were race-specific, suggesting that the biological effects of chronic psychosocial stress might differ among population groups. Third, pathway analyses revealed convergence on a few biologically relevant networks, including white adipose tissue browning, opioid signaling, and calcium signaling pathways, despite limited overlap at the individual CpG level. Finally, the overlap between psychosocial stress-related loci and loci previously linked to diabetes, cardiovascular disease, inflammation, and renal disease suggests that epigenetic changes may be one mechanism by which psychosocial stress influences chronic disease risk and health disparities.

One of the major gaps in our understanding of age-related metabolic and chronic disease is the identification of the biologic transduction pathways through which environmental stressors and social factors influence the risk of disease. Our data suggest DNAm is likely one of the biological pathways involved. Identifying differential DNAm patterns and genes associated with PD in population groups highlights the biological effect of social adversities such as PD on health outcomes in White and African American adults. We have identified differential methylation in specific CpGs within genes whose functions are central to disease and conditions that have been linked to exposure to discrimination, dementia, cancer, cardiovascular disease, renal disease, diabetes, and obesity. We also identified important molecular pathways through which discrimination stress may increase disease risk providing potential targets for further research and interventions to improve the health outcomes of all Americans.

## Materials and methods

### The HANDLS cohort

The Healthy Aging in Neighborhoods of Diversity across the Life Span (HANDLS) study is a population-based longitudinal study initiated in 2004 designed to disentangle the relationship between self-identified race and socioeconomic status in age-related health disparities. HANDLS is a fixed cohort of 3720 community-dwelling participants initially aged 30–64 years old who self-identified as either African American or White. The study includes participants recruited from 13 pre-determined neighborhoods in Baltimore, MD, USA using area probability sampling based on data from the US Census 2000 as described previously [46]. Participants were recruited using a four-way factorial cross of 5-year age groups, sex, race, and poverty status. Race was self-reported as either African American or White. Poverty status was determined by reported household income and categorized as above or below the 125% Federal Poverty Line as determined by the US Department of Health and Human Services in 2004.

### HANDLS DNA methylation cohort

This cohort included participants who had blood DNA available from the initial visit during 2004–9. As previously described [47, 48], 508 participants were randomly sampled using a factorial design across race, sex, and poverty status. Ultimately, 487 had DNAm data that passed the quality control, of which 467 had discrimination scale data available.

### Ethics

All participants of the HANDLS study provided written informed consent. The HANDLS study is approved by the National Institutes of Health Institutional Review Board. Protocol number: 09-AG-N248.

### Perceived discrimination measures

We employed six psychosocial stress measures in the present study: (i) sources of discrimination (Sdisc) [49], a 10-item inventory assessing experiences of discrimination based on gender, race, ethnicity, income, age, religion, physical appearance, sexual orientation, health status, and disability using a four-point scale ranging from 1 (not at all) to 4 (a lot); (ii) lifetime discrimination burden (Ldisc) [50], a two-item inventory assessing overall lifetime difficulties experienced due to discrimination using a four-point scale ranging from 1 (not at all) to 4 (a lot); (iii) gender discrimination (Gdisc) [19], a five-item inventory assessing gender discrimination experienced at school, at work, seeking employment, searching for housing, receiving medical care, and by police and courts using a binary response (no vs. yes); (iv) racial discrimination (Rdisc) [19], a six-item inventory assessing racial discrimination experienced at school, at work, seeking employment, searching for housing, receiving medical care, and by police and courts using a binary response (no vs. yes); (v) everyday discrimination (Edisc) [51], a nine-item inventory assessing the frequency of daily experiences with bias unrelated to race or ethnicity using a six-point scale ranging from 1 (almost every day) to

6 (never); and (vi) coping with discrimination (Cdisc), a four-item inventory assessing discrimination coping strategies using a binary response (yes vs. no) [19, 52]. Further details concerning, these scales were published previously [7]. We applied the Shapiro–Wilk normality test [53, 54] to these scales using the R package mvShapiroTest (https://cran.rproject.org/web/packages/mvShapiroTest/index.html).

## DNA methylation quantification

We used 250 ng of DNA isolated from blood from each participant sample, and DNA was treated with sodium bisulfate using a Zymo EZ-96 DNAm kit according to the manufacturer's protocol (ZYMO Research, Orange, CA, USA). We followed the standard protocols provided by the manufacturer for all kits with the suggested input/elution volumes [55]. After the bisulfate treatment, we performed genome-wide DNAm analysis using Illumina Infinium HumanMethylation EPIC BeadChip, the latest version of EPIC that efficiently quantifies the methylation of 866 836 CpG sites on the human genome [56, 57]

## Quality control and normalization

Respective IDAT files generated from the DNAm quantification were subjected to quality control and data preprocessing using the Bioconductor package *minfi* [58]. Data analysis of the samples that passed quality control was performed in R by integrating *minfi* [58], limma [59], *missMethyl* [60, 61], *IlluminaHumanMethylationEPICanno.ilm10b2.hg19* [61], and *IlluminaHumanMethylationEPICmanifest* [62] using raw methylation values. Background correction, dye-bias equalization, and normalization of the $\beta$ scores were performed using the normal-exponential out-of-band correction method [63] in the *minfi* package used to perform background correction, dye-bias equalization, and normalization of the $\beta$ scores. Single nucleotide polymorphisms (SNPs) associated probes were removed using the function *dropLociWithSnps* in *minfi* [58], which drops the probes that contain a SNP at the CpG interrogation or the single nucleotide extension. Technical variabilities in methylation measurements and batch effects from the plate were removed using *ComBat* [64].

## Association analysis of DNAm and psychosocial stress scales

To test the association between methylation at CpG sites across the genome and the different psychosocial stress scales (Sdisc, Rdisc, Ldisc, Gdisc, Edisc, Cdisc), we used the *cpg.assoc* function in *CpGassoc* package [65] implemented in R available at Barfield, R., Conneely, K., Kilaru, V (2024). _CpGassoc: Association Between Methylation and a Phenotype of Interest_. R package version 2.70, <https://CRANR-project.org/package=CpGassoc>.

Scale scores were log transformed if they were not normally distributed according to the results of the Shapiro–Wilk normality test (Ldisc and Rdisc). We performed an EWAS using *CpGassoc package* separately for African American and White participants to determine whether CpG sites are differentially methylated among the participants who reported lifetime discrimination compared to those who did not. We used multivariable linear regression to model the relationship between DNAm levels and psychosocial stress burden in each scale with age, sex, and poverty status with expected −log10(*P*-values) versus observed using the following models: Model 1 CpG ~ Lifetime discrimination (Ldisc) + age, Model 2 CpG ~ Lifetime discrimination (Ldisc) + sex, Model 3 CpG ~ Lifetime discrimination (Ldisc) + poverty status, and Model 4 CpG ~ Lifetime discrimination (Ldisc) + age + sex + poverty status. These models were examined on African American and White participants separately. We applied Holm–Bonferroni correction for multiple testing to the results for each discrimination scale. Significant results were determined using a false discovery rate of $< 0.05$.

Leukocyte cell-type proportions were estimated using the EstimateCellCounts() function in the minfi package with the FlowSorted.Blood.EPIC reference panel, a library for reference-based deconvolution of whole-blood biospecimens to estimate the composition of cell types assayed using the Illumina HumanMethylationEPIC BeadArray [66]. A major limitation of our study is that the estimated cell-type fractions were not included in the primary EWAS models because psychosocial stress may influence immune-cell composition, and adjustment could potentially remove biologically relevant variation that may lie on the causal pathway linking psychosocial stress exposure and DNAm.

## Identification of significant differentially methylated positions

The methylation level for each CpG site was estimated based on $\beta$ values ranging from 0 (the CpG site is unmethylated) to 1 (the CpG site is fully methylated). Initially, DMPs were estimated for the overall population agnostic to self-identified race using the *dmpFinder* function in the *minfi* package [58] for all discrimination scales. Using a linear regression test for continuous phenotypes, the *dmpFinder* function computes association between the methylation and a phenotype of interest. Identified DMPs from the *dmpFinder* function were prioritized using the following criteria: (i) a *P*-value $< .05$, indicating nominal association with each phenotype of interest; (ii) a $\Delta$beta value of $\pm 0.1$, signifying a relatively large differential methylation, as previously described [47, 67]. We also performed a race-stratified DMP analysis for the Ldisc scale to identify race-specific DMPs in African American and White study participants. We used these DMPs to identify overlaps between our discrimination data and previously identified DMPs and CpGs associated with PD, inflammation, diabetes, blood pressure, renal function decline, and inflammation. We found these previously identified DMPs and CpGs by conducting a targeted but not systematic literature review of studies that examined DNAm among minoritized populations in the context of PD assessed by the same instruments used in our study and health conditions associated with health disparities found in high frequency in our middle-aged African American and White adults. To identify the significant DMPs, we used the cut-off *P*-values $< .05$ and $< .01$.

## Functional pathway identification

We performed a Venn diagram comparison using the Venny 2.1.0 tool available at https://bioinfogp.cnb.csic.es/tools/venny/ to obtain the common and unique CpG sites that were associated significantly with each of the psychosocial stress scales. We uploaded the list of significantly differentially methylated CpG sites that were unique for each psychosocial stress scale for the covariates age, sex, poverty status, age + sex, and age + sex + poverty status containing gene identifiers and corresponding *P*-values obtained from *cpg.assoc*, into the IPA software (Qiagen). We performed the "core analysis" function included in the software to interpret biological processes,

canonical pathways, upstream transcriptional regulators, gene networks, diseases, and functions for each CpG site significant for each psychosocial stress scale. Each gene identifier for the CpG site was mapped to its corresponding gene object in the Ingenuity Pathway Knowledge Base (IPKB). Networks were drawn based on the IPA-IPKB (https://digitalinsights.qiagen.com/IPA).

## Acknowledgments

We thank the HANDLS medical staff for their careful evaluation of HANDLS participants and for obtaining the blood samples. We thank Althaf Lohani for technical assistance and the HANDLS participants for their continued participation in the study. This work utilized the computational resources of the NIH HPC Biowulf cluster (http://hpc.nih.gov). IPA analysis was conducted using the Temple University Computational Cluster.

## Author contributions

Kumaraswamy Naidu Chitrala (Conceptualization [equal], Formal Analysis [lead], Investigation [lead], Methodology [lead], Writing – original draft [equal], Writing – review & editing [equal]), Danielle L Beatty Moody (Conceptualization [equal], Data curation [equal], Writing – review & editing [equal]), Nicolle A. Mode (Data curation [equal], Formal Analysis [equal], Writing – review & editing [equal]), Botong Shen (Formal Analysis [equal], Methodology [supporting], Writing – review & editing [equal]), Nicole Noren Hooten (Methodology [equal], Visualization [equal], Writing – original draft [equal], Writing – review & editing [equal]), Alan B Zonderman (Data curation [equal], Formal Analysis [equal], Investigation [equal], Methodology [equal], Project administration [equal], Writing – original draft [equal], Writing – review & editing [equal]), Ngozi Ezike (Data curation [equal], Investigation [equal], Methodology [supporting], Writing – original draft [supporting]), and Michele Kim Evans (Conceptualization [lead], Funding acquisition [equal], Methodology [equal], Project administration [equal], Resources [lead], Supervision [lead], Writing – original draft [equal], Writing – review & editing [equal])

## Supplementary material

Supplementary material is available at *EnvEpig* online.

## Conflicts of interest

None declared.

## Funding

This research was supported [in part] by the Intramural Research Program of the National Institutes of Health (NIH). This project was funded by the Intramural Research Program of the National Institute on Aging (NIA), the National Institutes of Health (NIH), Baltimore, MD, project numbers AG000519 and AG000988. The contributions of the NIH author(s) are considered Works of the United States Government. The findings and conclusions presented in this paper are those of the author(s) and do not necessarily reflect the views of the NIH or the U.S. Department of Health and Human Services.

## Data Availability

Data are available to researchers after approval of a research proposal and after they have agreed to confidentiality as required by the National Institutes of Health Institutional Review Board. Policies and forms are available at: https://handls.nih.gov.

## References

1. Williams DR, Lawrence JA, Davis BA *et al.* Understanding how discrimination can affect health. *Health Serv Res* 2019;**54**:1374–88. https://doi.org/10.1111/1475-6773.13222
2. Lewis TT, Cogburn CD, Williams DR. Self-reported experiences of discrimination and health: scientific advances, ongoing controversies, and emerging issues. *Annu Rev Clin Psychol* 2015;**11**:407–40. https://doi.org/10.1146/annurev-clinpsy-032814-112728
3. Lockwood KG, Marsland AL, Matthews KA *et al.* Perceived discrimination and cardiovascular health disparities: a multisystem review and health neuroscience perspective. *Ann N Y Acad Sci* 2018;**1428**:170–207. https://doi.org/10.1111/nyas.13939
4. Whitaker KM, Everson-Rose SA, Pankow JS *et al.* Experiences of discrimination and incident type 2 diabetes mellitus: the Multi-Ethnic Study of Atherosclerosis (MESA). *Am J Epidemiol* 2017;**186**:445–55. https://doi.org/10.1093/aje/kwx047
5. Barnes LL, Lewis TT, Begeny CT *et al.* Perceived discrimination and cognition in older African Americans. *J Int Neuropsychol Soc* 2012;**18**:856–65. https://doi.org/10.1017/S1355617712000628
6. Zahodne LB, Kraal AZ, Sharifian N *et al.* Inflammatory mechanisms underlying the effects of everyday discrimination on age-related memory decline. *Brain Behav Immun* 2019;**75**:149–54. https://doi.org/10.1016/j.bbi.2018.10.002
7. Beatty Moody DL, Taylor AD, Leibel DK *et al.* Lifetime discrimination burden, racial discrimination, and subclinical cerebrovascular disease among African Americans. *Health Psychol* 2019;**38**:63–74. https://doi.org/10.1037/hea0000638
8. Ruiz-Narváez EA, Cozier Y, Zirpoli G *et al.* Perceived experiences of racism in relation to genome-wide DNA methylation and epigenetic aging in the Black Women's Health Study. *J Racial Ethn Health Disparities* 2025;**12**:754–63. https://doi.org/10.1007/s40615-024-01915-3
9. Zhao W, Lin L, Kelly KM *et al.* Epigenome-wide association study of perceived discrimination in the Multi-Ethnic Study of Atherosclerosis (MESA). *Epigenetics* 2025;**20**:2445447. https://doi.org/10.1080/15592294.2024.2445447
10. Alegria-Torres JA, Baccarelli A, Bollati V. Epigenetics and lifestyle. *Epigenomics* 2011;**3**:267–77. https://doi.org/10.2217/epi.11.22
11. Peters A, Nawrot TS, Baccarelli AA. Hallmarks of environmental insults. *Cell* 2021;**184**:1455–68. https://doi.org/10.1016/j.cell.2021.01.043
12. Palma-Gudiel H, Fananas L, Horvath S *et al.* Psychosocial stress and epigenetic aging. *Int Rev Neurobiol* 2020;**150**:107–28. https://doi.org/10.1016/bs.irn.2019.10.020
13. Keil KP, Lein PJ. DNA methylation: a mechanism linking environmental chemical exposures to risk of autism spectrum disorders? *Environ Epigenet* 2016;**2**:dvv012. https://doi.org/10.1093/eep/dvv012
14. Binder DSE. (eds).Spengler D, Binder E , *Epigenetics and Neuroendocrinology Clinical Focus on Psychiatry*. vol **2**. Cham: Springer International Publishing, 2016.
15. Brody GH, Miller GE, Yu T *et al.* Supportive family environments ameliorate the link between racial discrimination and epigenetic

aging: a replication across two longitudinal cohorts. *Psychol Sci* 2016;**27**:530–41. https://doi.org/10.1177/0956797615626703
16. Barcelona de Mendoza V, Huang Y, Crusto CA *et al.* Perceived racial discrimination and DNA methylation among African American women in the InterGEN study. *Biol Res Nurs* 2018;**20**:145–52. https://doi.org/10.1177/1099800417748759
17. Santos HP, Jr., Nephew BC, Bhattacharya A *et al.* Discrimination exposure and DNA methylation of stress-related genes in Latina mothers. *Psychoneuroendocrinology* 2018;**98**:131–38. https://doi.org/10.1016/j.psyneuen.2018.08.014
18. van der Laan LC, Meeks KAC, Chilunga FP *et al.* Epigenome-wide association study for perceived discrimination among sub-Saharan African migrants in Europe—the RODAM study. *Sci Rep* 2020;**10**:4919. https://doi.org/10.1038/s41598-020-61649-0
19. Krieger N. Racial and gender discrimination: risk factors for high blood pressure? *Soc Sci Med* 1990;**30**:1273–81. https://doi.org/10.1016/0277-9536(90)90307-e
20. Williams DR, Mohammed SA. Discrimination and racial disparities in health: evidence and needed research. *J Behav Med* 2009;**32**:20–47. https://doi.org/10.1007/s10865-008-9185-0
21. Forde AT, Lewis TT, Kershaw KN *et al.* Perceived discrimination and hypertension risk among participants in the Multi-Ethnic Study of Atherosclerosis. *J Am Heart Assoc* 2021;**10**:e019541. https://doi.org/10.1161/JAHA.120.019541
22. Brown KM, Hui Q, Huang Y *et al.* Association between stress and coping with DNA methylation of blood pressure-related genes among African American women. *Chronic Stress (Thousand Oaks)* 2019;**3**. https://doi.org/10.1177/2470547019879088
23. Taylor JY, Wright ML, Crusto CA *et al.* The Intergenerational Impact of Genetic and Psychological Factors on Blood Pressure (InterGEN) study: design and methods for complex DNA analysis. *Biol Res Nurs* 2016;**18**:521–30. https://doi.org/10.1177/1099800416645399
24. Kho M, Zhao W, Ratliff SM *et al.* Epigenetic loci for blood pressure are associated with hypertensive target organ damage in older African Americans from the Genetic Epidemiology Network of Arteriopathy (GENOA) study. *BMC Med Genomics* 2020;**13**:131. https://doi.org/10.1186/s12920-020-00791-0
25. Ligthart S, Marzi C, Aslibekyan S *et al.* DNA methylation signatures of chronic low-grade inflammation are associated with complex diseases. *Genome Biol* 2016;**17**:255. https://doi.org/10.1186/s13059-016-1119-5
26. Qiu C, Hanson RL, Fufaa G *et al.* Cytosine methylation predicts renal function decline in American Indians. *Kidney Int* 2018;**93**:1417–31. https://doi.org/10.1016/j.kint.2018.01.036
27. Sharma NK, Comeau ME, Montoya D *et al.* Integrative analysis of glucometabolic traits, adipose tissue DNA methylation, and gene expression identifies epigenetic regulatory mechanisms of insulin resistance and obesity in African Americans. *Diabetes* 2020;**69**:2779–93. https://doi.org/10.2337/db20-0117
28. Lambert E, Saha O, Soares Landeira B *et al.* The Alzheimer susceptibility gene BIN1 induces isoform-dependent neurotoxicity through early endosome defects. *Acta Neuropathol Commun* 2022;**10**:4. https://doi.org/10.1186/s40478-021-01285-5
29. Hu H, Tan L, Bi YL *et al.* Association between methylation of BIN1 promoter in peripheral blood and preclinical Alzheimer's disease. *Transl Psychiatry* 2021;**11**:89. https://doi.org/10.1038/s41398-021-01218-9
30. Chi J, Cohen P. The multifaceted roles of PRDM16: adipose biology and beyond. *Trends Endocrinol Metab* 2016;**27**:11–23. https://doi.org/10.1016/j.tem.2015.11.005
31. Stepanikova I, Baker EH, Simoni ZR *et al.* The role of perceived discrimination in obesity among African Americans. *Am J Prev Med* 2017;**52**:S77–85. https://doi.org/10.1016/j.amepre.2016.07.034
32. Zhang L, Zhou A, Zhu S *et al.* The role of GTPase-activating protein ARHGAP26 in human cancers. *Mol Cell Biochem* 2022;**477**:319–26. https://doi.org/10.1007/s11010-021-04274-3
33. Pommier Y, Nussenzweig A, Takeda S *et al.* Human topoisomerases and their roles in genome stability and organization. *Nat Rev Mol Cell Biol* 2022;**23**:407–27. https://doi.org/10.1038/s41580-022-00452-3
34. Cypess AM. Reassessing human adipose tissue. *N Engl J Med* 2022;**386**:768–79. https://doi.org/10.1056/NEJMra2032804
35. Claro V, Ferro A. Netrin-1: focus on its role in cardiovascular physiology and atherosclerosis. *JRSM Cardiovasc Dis* 2020;**9**:2048004020959574. https://doi.org/10.1177/2048004020959574
36. Bruikman CS, Vreeken D, Hoogeveen RM *et al.* Netrin-1 and the grade of atherosclerosis are inversely correlated in humans. *Arterioscler Thromb Vasc Biol* 2020;**40**:462–72. https://doi.org/10.1161/ATVBAHA.119.313624
37. Bruikman CS, Zhang H, Kemper AM *et al.* Netrin family: role for protein isoforms in cancer. *J Nucleic Acids* 2019;**2019**:3947123. https://doi.org/10.1155/2019/3947123
38. Stein C. Opioid receptors. *Annu Rev Med* 2016;**67**:433–51. https://doi.org/10.1146/annurev-med-062613-093100
39. Eisenstein TK. The role of opioid receptors in immune system function. *Front Immunol* 2019;**10**:2904. https://doi.org/10.3389/fimmu.2019.02904
40. Cissom C, J JP, Shariat-Madar Z. Dynorphins in development and disease: implications for cardiovascular disease. *Curr Mol Med* 2020;**20**:259–74. https://doi.org/10.2174/1566524019666191028122559
41. Martin C, Cho YE, Kim H *et al.* Altered DNA methylation patterns associated with clinically relevant increases in PTSD symptoms and PTSD symptom profiles in military personnel. *Biol Res Nurs* 2018;**20**:352–58. https://doi.org/10.1177/1099800418758951
42. Blackwood CA, Cadet JL. Epigenetic and genetic factors associated with opioid use disorder: are these relevant to African American populations. *Front Pharmacol* 2021;**12**:798362. https://doi.org/10.3389/fphar.2021.798362
43. Grandin M, Mathot P, Devailly G *et al.* Inhibition of DNA methylation promotes breast tumor sensitivity to netrin-1 interference. *EMBO Mol Med* 2016;**8**:863–77. https://doi.org/10.15252/emmm.201505945
44. Machado SA, Pasquarelli-do-Nascimento G, da Silva DS *et al.* Browning of the white adipose tissue regulation: new insights into nutritional and metabolic relevance in health and diseases. *Nutr Metab (Lond)* 2022;**19**:61. https://doi.org/10.1186/s12986-022-00694-0
45. Lucchini FC, Wueest S, Challa TD *et al.* ASK1 inhibits browning of white adipose tissue in obesity. *Nat Commun* 2020;**11**:1642. https://doi.org/10.1038/s41467-020-15483-7
46. Evans MK, Lepkowski JM, Powe NR *et al.* Healthy aging in neighborhoods of diversity across the life span (HANDLS): overcoming barriers to implementing a longitudinal, epidemiologic, urban study of health, race, and socioeconomic status. *Ethn Dis* 2010; **20**:267–75.
47. Chitrala KN, Hernandez DG, Nalls MA *et al.* Race-specific alterations in DNA methylation among middle-aged African Americans and Whites with metabolic syndrome. *Epigenetics* 2020;**15**:462–82. https://doi.org/10.1080/15592294.2019.1695340
48. Tajuddin SM, Hernandez DG, Chen BH *et al.* Novel age-associated DNA methylation changes and epigenetic age acceleration in

middle-aged African Americans and Whites. *Clin Epigenetics* 2019;**11**:119. https://doi.org/10.1186/s13148-019-0722-1
49. LaVeist TA, Rolley NC, Diala C. Prevalence and patterns of discrimination among U.S. health care consumers. *Int J Health Serv* 2003;**33**:331–44. https://doi.org/10.2190/TCAC-P90F-ATM5-B5U0
50. Friedman EM, Williams DR, Singer BH *et al.* Chronic discrimination predicts higher circulating levels of E-selectin in a national sample: the MIDUS study. *Brain Behav Immun* 2009;**23**:684–92. https://doi.org/10.1016/j.bbi.2009.01.002
51. Williams DR, Yan Y, Jackson JS *et al.* Racial differences in physical and mental health: socio-economic status, stress and discrimination. *J Health Psychol* 1997;**2**:335–51. https://doi.org/10.1177/135910539700200305
52. McNeilly MD, Anderson NB, Armstead CA *et al.* The perceived racism scale: a multidimensional assessment of the experience of White racism among African Americans. *Ethn Dis* 1996; **6**:154–66.
53. Royston P. An extension of Shapiro and Wilk's W test for normality to large samples. *J R Stat Soc Ser C Appl Stat* 1982;**31**:115–24.
54. Royston P. Remark AS R94: a remark on Algorithm AS 181: the W test for normality. *J R Stat Soc Ser C Appl Stat* 1995;**44**:547–51.
55. Kint S, De Spiegelaere W, De Kesel J *et al.* Evaluation of bisulfite kits for DNA methylation profiling in terms of DNA fragmentation and DNA recovery using digital PCR. *PLoS One* 2018;**13**:e0199091. https://doi.org/10.1371/journal.pone.0199091
56. Moran S, Arribas C, Esteller M. Validation of a DNA methylation microarray for 850,000 CpG sites of the human genome enriched in enhancer sequences. *Epigenomics* 2016;**8**:389–99. https://doi.org/10.2217/epi.15.114
57. Pidsley R, Zotenko E, Peters TJ *et al.* Critical evaluation of the Illumina MethylationEPIC BeadChip microarray for whole-genome DNA methylation profiling. *Genome Biol* 2016;**17**:208. https://doi.org/10.1186/s13059-016-1066-1
58. Aryee MJ, Jaffe AE, Corrada-Bravo H *et al.* Minfi: a flexible and comprehensive Bioconductor package for the analysis of Infinium DNA methylation microarrays. *Bioinformatics* 2014;**30**:1363–69. https://doi.org/10.1093/bioinformatics/btu049
59. Smyth GK. Limma: linnear models for microarray data. In: Gentelman R, Carey VJ, Huber W, Irizarry RA, Dudoit S (eds.), *Bioinformatics and Computational Biology Solutions Using R and Bioconductor Statistics for Biology and Health*. New York, NY: Springer, 2005.
60. Phipson B, Maksimovic J, Oshlack A. missMethyl: an R package for analyzing data from Illumina's HumanMethylation450 platform. *Bioinformatics* 2016;**32**:286–88. https://doi.org/10.1093/bioinformatics/btv560
61. Hansen KD. Annotation for Illumina's EPIC methylation arrays. R package version 0.6.0. Illumina Human Methylation EPIC annoilm10b2hg.
62. Hansen KD. Illumina Human Methylation EPIC manifest. Manifest for Illumina's EPIC methylation arrays R package version 030 Accessed 2019.
63. Triche TJ , Jr., Weisenberger DJ, Van Den Berg D, Laird PW *et al.* Low-level processing of Illumina Infinium DNA Methylation BeadArrays. *Nucleic Acids Res* 2013;**41**:e90. https://doi.org/10.1093/nar/gkt090
64. Johnson WE, Li C, Rabinovic A. Adjusting batch effects in microarray expression data using empirical Bayes methods. *Biostatistics* 2007;**8**:118–27. https://doi.org/10.1093/biostatistics/kxj037
65. Barfield RT, Kilaru V, Smith AK *et al.* CpGassoc: an R function for analysis of DNA methylation microarray data. *Bioinformatics* 2012;**28**:1280–81. https://doi.org/10.1093/bioinformatics/bts124
66. Salas LA, Koestler DC, Butler RA *et al.* An optimized library for reference-based deconvolution of whole-blood biospecimens assayed using the Illumina HumanMethylationEPIC BeadArray. *Genome Biol* 2018;**19**:64. https://doi.org/10.1186/s13059-018-1448-7
67. Maltby VE, Lea RA, Sanders KA *et al.* Differential methylation at MHC in CD4(+) T cells is associated with multiple sclerosis independently of HLA-DRB1. *Clin Epigenetics* 2017;**9**:71. https://doi.org/10.1186/s13148-017-0371-1
68. Liu X, Xie H, Fu Z *et al.* MAD1L1 and TSNARE gene polymorphisms are associated with schizophrenia susceptibility in the Han Chinese population. *BMC Med Genomics* 2021;**14**:218. https://doi.org/10.1186/s12920-021-01070-2
69. Vitalle J, Terren I, Gamboa-Urquijo L *et al.* Altered expression of CD300a inhibitory receptor on CD4+ T cells from human immunodeficiency virus-1-infected patients: association with disease progression markers. *Front Immunol* 2018;**9**:1709. https://doi.org/10.3389/fimmu.2018.01709
70. Lee S. The association of genetically controlled CpG methylation (cg158269415) of protein tyrosine phosphatase, receptor type N2 (PTPRN2) with childhood obesity. *Sci Rep* 2019;**9**:4855. https://doi.org/10.1038/s41598-019-40486-w
71. Jordan VK, Fregeau B, Ge X *et al.* Genotype–phenotype correlations in individuals with pathogenic RERE variants. *Hum Mutat* 2018;**39**:666–75. https://doi.org/10.1002/humu.23400
72. Wang K, Lu Y, Morrow DF *et al.* Alzheimer's disease neuroimaging I. Associations of ARHGAP26 polymorphisms with Alzheimer's disease and cardiovascular disease. *J Mol Neurosci* 2022;**72**:1085–97. https://doi.org/10.1007/s12031-022-01972-5
73. Mavioglu RN, Kara B, Akansel G *et al.* FAM160B1 deficit associated with microcephaly, severe intellectual disability, ataxia, behavioral abnormalities and speech problems. *Clin Genet* 2019;**96**:456–60. https://doi.org/10.1111/cge.13612
74. Marbach F, Stoyanov G, Erger F *et al.* Variants in PRKAR1B cause a neurodevelopmental disorder with autism spectrum disorder, apraxia, and insensitivity to pain. *Genet Med* 2021;**23**:1465–73. https://doi.org/10.1038/s41436-021-01152-7
75. Moroy T, Khandanpour C. Role of GFI1 in epigenetic regulation of MDS and AML pathogenesis: mechanisms and therapeutic implications. *Front Oncol* 2019;**9**:824. https://doi.org/10.3389/fonc.2019.00824
76. Cibi DM, Bi-Lin KW, Shekeran SG *et al.* Prdm16 deficiency leads to age-dependent cardiac hypertrophy, adverse remodeling, mitochondrial dysfunction, and heart failure. *Cell Rep* 2020;**33**:108288. https://doi.org/10.1016/j.celrep.2020.108288
77. Bonner SM, Pietropaolo SL, Fan Y *et al.* Sequence variation in promoter of Ica1 gene, which encodes protein implicated in type 1 diabetes, causes transcription factor autoimmune regulator (AIRE) to increase its binding and down-regulate expression. *J Biol Chem* 2012;**287**:17882–93. https://doi.org/10.1074/jbc.M111.319020
78. Schwarz A, Moller-Hackbarth K, Ebarasi L *et al.* Coro2b, a podocyte protein downregulated in human diabetic nephropathy, is involved in the development of protamine sulphate-induced foot process effacement. *Sci Rep* 2019;**9**:8888. https://doi.org/10.1038/s41598-019-45303-y
79. Jahan Z, Benthani FA, Currey N *et al.* MCC gene silencing is a CpG island methylator phenotype-associated factor that predisposes colon cancer cells to irinotecan and olaparib. *Cancers* 2022; **14**:2859. https://doi.org/10.3390/cancers14122859

80. Meeks KAC, Henneman P, Venema A *et al.* Epigenome-wide association study in whole blood on type 2 diabetes among sub-Saharan African individuals: findings from the RODAM study. *Int J Epidemiol* 2019;**48**:58–70. https://doi.org/10.1093/ije/dyy171
81. Houfaf Khoufaf FZ, Sanchez A, Idrissou M *et al.* Role of UTX histone demethylase in regulation of MGMT, TRA2A, U2AF1, and RPS6KA2 genes in prostate cancer cell lines. *Omics* 2021;**25**:129–31. https://doi.org/10.1089/omi.2020.0183
82. Xu G, Zhu H, Xu J *et al.* Long non-coding RNA POU6F2-AS2 promotes cell proliferation and drug resistance in colon cancer by regulating miR-377/BRD4. *J Cell Mol Med* 2020;**24**:4136–49. https://doi.org/10.1111/jcmm.15070
83. Zhang Z, Yin J, Lu C *et al.* Exosomal transfer of long non-coding RNA SBF2-AS1 enhances chemoresistance to temozolomide in glioblastoma. *J Exp Clin Cancer Res* 2019;**38**:166. https://doi.org/10.1186/s13046-019-1139-6
84. Klemp I, Hoffmann A, Muller L *et al.* DNA methylation patterns reflect individual's lifestyle independent of obesity. *Clin Transl Med* 2022;**12**:e851. https://doi.org/10.1002/ctm2.851
85. Li J, Xu H, Wang Q *et al.* Pard3 suppresses glioma invasion by regulating RhoA through atypical protein kinase C/NF-kappaB signaling. *Cancer Med* 2019;**8**:2288–302. https://doi.org/10.1002/cam4.2063
86. Kumar P, Gogulamudi VR, Periasamy R *et al.* Inhibition of HDAC enhances STAT acetylation, blocks NF-kappaB, and suppresses the renal inflammation and fibrosis in Npr1 haplotype male mice. *Am J Physiol Renal Physiol* 2017;**313**:F781–95. https://doi.org/10.1152/ajprenal.00166.2017
87. Feng L, Zhao K, Sun L *et al.* SLC7A11 regulated by NRF2 modulates esophageal squamous cell carcinoma radiosensitivity by inhibiting ferroptosis. *J Transl Med* 2021;**19**:367. https://doi.org/10.1186/s12967-021-03042-7
88. Aldaz CM, Hussain T. WWOX loss of function in neurodevelopmental and neurodegenerative disorders. *Int J Mol Sci* 2020;**21**:8922. https://doi.org/10.3390/ijms21238922
89. Zhang Z, Liu X, Huang R *et al.* Upregulation of nucleoprotein AHNAK is associated with poor outcome of pancreatic ductal adenocarcinoma prognosis via mediating epithelial-mesenchymal transition. *J Cancer* 2019;**10**:3860–70. https://doi.org/10.7150/jca.31291
90. Ashktorab H, Daremipouran M, Goel A *et al.* DNA methylome profiling identifies novel methylated genes in African American patients with colorectal neoplasia. *Epigenetics* 2014;**9**:503–12. https://doi.org/10.4161/epi.27644
91. Hong JY, Kim HJ, Kim K *et al.* TPK1 as a predictive marker for the anti-tumour effects of simvastatin in gastric cancer. *Pathol Res Pract* 2020;**216**:152820. https://doi.org/10.1016/j.prp.2020.152820
92. Wang J, Huang R, Huang Y *et al.* Overexpression of NOP58 as a prognostic marker in hepatocellular carcinoma: a TCGA data-based analysis. *Adv Ther* 2021;**38**:3342–61. https://doi.org/10.1007/s12325-021-01762-2
93. Wang C, Li L, Yin Z *et al.* An indel polymorphism within pre-miR3131 confers risk for hepatocellular carcinoma. *Carcinogenesis* 2017;**38**:168–76. https://doi.org/10.1093/carcin/bgw206
94. Brown TC, Juhlin CC, Healy JM *et al.* DNA copy amplification and overexpression of SLC12A7 in adrenocortical carcinoma. *Surgery* 2016;**159**:250–58. https://doi.org/10.1016/j.surg.2015.08.038
95. Yang J, Ma Q, Dincheva I *et al.* SorCS2 is required for social memory and trafficking of the NMDA receptor. *Mol Psychiatry* 2021;**26**:927–40. https://doi.org/10.1038/s41380-020-0650-7
96. Koenig SN, Sucharski HC, Jose EM *et al.* Inherited variants in SCARB1 cause severe early-onset coronary artery disease. *Circ Res* 2021;**129**:296–307. https://doi.org/10.1161/CIRCRESAHA.120.318793
97. Cristiano L. The pseudogenes of eukaryotic translation elongation factors (EEFs): role in cancer and other human diseases. *Genes Dis* 2022;**9**:941–58. https://doi.org/10.1016/j.gendis.2021.03.009
98. McLachlan F, Sires AM, Abbott CM. The role of translation elongation factor eEF1 subunits in neurodevelopmental disorders. *Hum Mutat* 2019;**40**:131–41. https://doi.org/10.1002/humu.23677
99. Lee RG, Sedghi M, Salari M *et al.* Early-onset Parkinson disease caused by a mutation in CHCHD2 and mitochondrial dysfunction. *Neurol Genet* 2018;**4**:e276. https://doi.org/10.1212/NXG.0000000000000276




**Received:** 11 September 2025. **Revised:** 31 July 2026. **Accepted:** 9 August 2026